Mendelian randomization combined with single-cell sequencing data analysis of chemokines and chemokine receptors and key genes and molecular mechanisms associated with epilepsy

Lin-Ming Zhang[a,*], Tao Zeng[b,*], Bing-ran Zhang[c,*], Qiu-juan Zhang[c], Shu-ji Gao[c], Yan-lin Zhu[c] and Ming-wei Liu[d]

Objective **To explore the functions and potential regulatory mechanisms of chemokine and chemokine receptor (CCR)-related genes in epilepsy.**

Methods **CCRs were identified as candidate genes and their causal relationship with epilepsy was rigorously evaluated via Mendelian randomization analysis. Subsequently, single-cell RNA sequencing (scRNA-seq) data were analyzed to identify and classify cell clusters into distinct types based on cellular annotation. Differential expression analysis was conducted to pinpoint key genes by overlapping the candidate gene set with differentially expressed genes (DEGs). Furthermore, potential therapeutic drugs for epilepsy were predicted, offering novel avenues for disease management and treatment.**

Results **In total, 6395 DEGs were identified across the six cell clusters. After their intersection, CCRL2, XCL2, CXCR5, CXCL1, and CX3CR1 were pinpointed as key genes. Microglia, T cells, B cells, and macrophages have been emerged as critical cells. Furthermore, CXCL1 was regulated by hsa-miR-570-3p and hsa-miR-532-5p. Notably, CXCR5, CXCL1, and CX3CR1 were associated with 27 drug compounds. This comprehensive study leveraged scRNA-seq and transcriptomic data to elucidate the roles of CCR-related genes in epilepsy. Notably, CCRL2, XCL2, CXCR5, CXCL1,and CX3CR1 were identified as key genes implicated in epilepsy, whereas microglia, T cells, B cells, and macrophages were recognized as critical contributors to the development of epilepsy.**

Conclusions **Regulating the expression of CCRL2, XCL2, CXCR5, CXCL1, and CX3CR1, along with the activity of these immune cells may offer therapeutic potential for the alleviation of epilepsy.** ***NeuroReport*** **36: 467–486**

NeuroReport 2025, **36**:467–486

Keywords: chemokine and chemokine receptors, epilepsy, Mendelian randomization analysis, single-cell RNA sequencing data

[a]Department of Neurology, The First Affiliated Hospital of Kunming Medical University, Kunming, Yunnan, China, [b]Department of Neurology, The Pearl River Hospital Affiliated to Southern Medical University, Guangzhou, Guangdong, China, [c]Department of Emergency, The First Affiliated Hospital of Kunming Medical University, Kunming, Yunnan, China and [d]Department of Emergency, Dali Bai Autonomous Prefecture People's Hospital, Dali, Yunnan, China

Correspondence to Ming-wei Liu, MD, Department of Emergency, Dali Bai Autonomous Prefecture People's Hospital, 35 Renmin South Road, Xiaguan Street, Dali, 671000, China
Tel: 86-15198852569; e-mail: lmw2004210@163.com

*Lin-Ming Zhang, Tao Zeng, and Bing-ran Zhang contributed equally to this work.

Received 3 October 2024 **Accepted** 26 February 2025.

Introduction

Epilepsy is a complex and heterogeneous chronic neurological disorder characterized by unprovoked seizures resulting from transient abnormal neuronal activity, ultimately contributing to neurocognitive impairment [1,2]. Epidemiological studies indicate that approximately 50 million individuals globally are affected by this disorder, with a notable increase in its incidence [3]. Individuals with epilepsy present with a diverse array of symptoms. These symptoms can encompass unusual sensations, emotions, and behaviors, seizures, muscle spasms, and loss of consciousness due to the brain sending erroneous signals [4]. Diagnosing epilepsy can be challenging due to its complexity and the existence of multiple subtypes [5]. Currently, the mainstay of epilepsy treatment is antiepileptic drug administration. The US Food and Drug Administration has approved over 20 antiepileptic drugs. However, up to one-third of individuals with epilepsy develop resistance to these medications [6,7].

Chemokines constitute a substantial class of small, secreted proteins that transmit signals via chemokine receptors, which are linked to G-proteins on the cellular surface. These proteins are pivotal in a wide array of biological and pathological processes, notably including cancer, as they regulate immune and inflammatory responses, as well as govern cell migration, proliferation, and survival [8]. To date, over 50 chemokines more

Supplemental Digital Content is available for this article. Direct URL citations appear in the printed text and are provided in the HTML and PDF versions of this article on the journal's website, www.neuroreport.com.

than 20 chemokine receptors have been identified. Based on the primary structure of their peptide chains, chemokines are categorized into four subfamilies: CC, CXC, XC, and CX3C. Similarly, typical chemokine receptors are divided into four subfamilies according to their specific ligand-binding characteristics: C-C motif chemokine receptor (CCR) (CCR1-CCR11) and CXCR (CXCR1-CXCR6) [9]. The CXCR5 chemokine receptor is involved in cell migration and localization, facilitating cell-cell interactions and exhibiting upregulation in epileptic brain tissue [10]. Notably, chemokines such as CCL2, CCL3, CCL4, and CCL5 are markedly upregulated in the hippocampus and other temporal lobe structures of patients with epilepsy [11]. Previous studies have demonstrated that the elevated expression of CCL2 in inflamed brains is intimately associated with the activation and subsequent recruitment of macrophages and microglia to the site of injury, thereby potentiating the inflammatory response [12]. Although genes coding for chemokines such as XCL2, CXCR5, and CX3CR1, along with the pathways they participate in, have been implicated in the etiology of epilepsy, the precise pathological mechanisms underlying their involvement remain elusive.

Research has uncovered a significant association between CCR and epilepsy, with enrichment scores tightly linked to key genes in multitranscriptome data. Furthermore, chemokines CCL3 and CCL4 are notably upregulated in chronic temporal lobe epilepsy (TLE), and this alteration is observable even in animal models during the early stages of the condition. This suggests that these chemokines may contribute to the progression of epilepsy by directly or indirectly modulating neuronal excitability and intensifying immune responses. In conclusion, CCR may represent a pivotal immune signaling pathway in the pathogenesis of epilepsy [13]. Research has shown that the chemokine protein family, secreted by astrocytes, microglia, and endothelial cells, regulates neuronal excitability and facilitates the entry of immune cells into the brain via G protein-coupled receptors. This regulation occurs via modulation of neurotransmitter release and voltage or G protein-dependent channels. In an animal model of epilepsy, chemokines and their receptors CCR2, CCR5, CXCR4, and CXCR5, including CCL2, CCL3, and fractalkine (CX3CL1), exhibited significant upregulation in the hippocampus. These findings underscore the crucial interplay between chemokines and their downstream signaling pathways in neuroinflammation and the pathogenesis of epilepsy [14–16]. Neuroinflammation, a pivotal regulatory factor in brain health, significantly promotes the onset and progression of epilepsy. In particular, heightened levels of pro-inflammatory cytokines (PICs), including interleukin-1β (IL-1β), IL-6, and tumor necrosis factor-alpha (TNF-α), have been closely linked to epileptic seizures. The excessive release of these cytokines not only intensifies neuronal excitability but also stimulates the activation of glial cells, thereby augmenting the inflammatory response. This process creates a vicious cycle that may ultimately heighten susceptibility to epilepsy and increase seizure frequency [17]. These studies indicate that chemokines play a crucial role in epilepsy development.

Therefore, this study integrated transcription data with single-cell RNA sequencing (scRNA-seq) to explore chemokine and chemokine receptor (CCR)-related genes in epilepsy, exploring their functions and potential regulatory mechanisms. By employing Mendelian randomization (MR) analysis, the study aimed to elucidate the causal relationship between CCR-related genes and epilepsy. This comprehensive approach aims to deepen our understanding of the pathogenesis of epilepsy and pave the way for novel therapeutic strategies for patients with this condition.

Methods

Associated data

The scRNA-seq data were downloaded from the gene expression omnibus database, specifically utilizing the GSE201048 dataset, which encompassed 85 780 single cells derived from epileptic brain tissues. Additionally, the GSE190452 dataset was used to validate prognostic genes, including three cases in the epilepsy group and normal control brain tissue samples. Immune cells were isolated and extracted from brain tissue samples of 11 patients diagnosed with epilepsy [18]. A total of 64 CCRs were obtained through an extensive literature review [19]. By integrating data from the Integrative Epidemiology Unit Open GWAS database (IEU OpenGWAS, https://gwas.mrcieu.ac.uk/), a Genome-wide association study (GWAS) and expression quantitative trait locus information for these 64CCRs (exposure factors) were assembled. Simultaneously, the trait ID (ukb-b-16309) for epilepsy was searched and downloaded as an outcome from the IEU open GWAS database, which encompasses samples from 3810 epilepsy patients and 459 123 controls, encompassing a total of 9 851 867 single nucleotide polymorphisms (SNPs). The sample included both male and female individuals from Europe.

Selection of instrumental variables

Univariable Mendelian randomization (UVMR) analysis of CCRs (exposure factors) and epilepsy (outcome) was conducted to investigate their causal relationship. During this analysis, three core assumptions of classical MR were rigorously upheld: 1. independence assumption (The causal relationship between CCRs and epilepsy is uninfluenced by confounding factors); 2. Association assumption [instrumental variables (IVs) must exhibit a strong correlation with CCRs]; 3. Exclusivity assumption (CCRs are the only pathway through which genetic variation can impact epilepsy). Immediately thereafter, the IVs satisfying the above

three key assumptions were screened. Utilizing the R package 'TwoSampleMR' (version 0.5.7) [20], the extracted instrument function was first utilized to read the exposure data, enabling the filtering of significant IVs that were tightly correlated with the exposure factor. Subsequently, the extract_outcome_data function was employed to read the outcome data. This step further screened the IVs to ensure they were not only associated with the exposure factor but also independent of the outcome data, yielding a collection of efficient and unbiased IVs ($P < 5 \times 10^{-6}$). To eliminate SNPs with linkage disequilibrium, the clump function was utilized with parameters set to clump = TRUE, $r^2 = 0.001$, kb = 10. Furthermore, the function extract_outcome_data function was used to identify SNPs that were not associated with the outcome. The strength of IVs was evaluated using the *F*-statistic, with the subsequent step proceeding only when the *F*-value exceeded 10. To ensure consistency, the harmonize_data function was employed to harmonize the effect alleles and effect sizes, aligning the alleles of each SNP across the relevant exposure factors and outcomes. Similarly, SNPs for the multivariable Mendelian randomization (MVMR) analysis were screened through this method.

Univariable Mendelian randomization analysis

The causal relationship between CCRs and epilepsy was evaluated through UVMR analysis. During this analysis, the causal link between the two was inferred using various methods, including inverse variance weighted (IVW) [21], weighted median [22], MR Egger [23], simple mode [24], and weighted mode [25] methods. In this case, the IVW served as the primary approach to test for causal effects. A statistically significant causal relationship between CCRs and epilepsy was established when the *P*-value derived from the IVW method was <0.05, signifying a strong correlation. Specifically, when the odds ratios (ORs) were greater than 1, CCRs were deemed risk factors for epilepsy. Conversely, ORs < 1 were interpreted as protective factors against epilepsy. Ultimately, the results of the UVMR analysis were visualized through the use of scatter plots, forest plots, and funnel plots.

Sensitivity analysis

We further evaluated the reliability of the UVMR results, and several tests were conducted, including assessments for heterogeneity, horizontal pleiotropy, and leave-one-out (LOO) analysis. Specifically, mr_heterogeneity was employed to examine whether heterogeneity was present in the analysis, with a *P*-value exceeding 0.05 suggesting the absence of heterogeneity. Additionally, mr_pleiotropy_test function was used to detect horizontal pleiotropy among SNPs, with a $P > 0.05$ indicating no horizontal pleiotropy among the SNPs. Then, the LOO test was conducted to assess the impact of each individual SNP on the outcome by sequentially excluding them. Furthermore, the Steiger test was performed to eliminate the possibility of reverse causation. When all SNPs related to CCRs showed a TRUE orientation and had $P < 0.05$, they successfully passed the Steiger test. Consequently, CCRs that demonstrated a causal link with epilepsy were selected as candidate genes for subsequent analyses.

Functional enrichment analysis of candidate genes and construction of a protein-protein interaction network

To gain insights into the biological functions and signaling pathways in which candidate genes are involved. The candidate genes were annotated for the Gene Ontology (GO) function and the Kyoto Encyclopedia of Genes and Genomes(KEGG) signaling pathway using 'clusterProfiler' (version 4.7.1.003) [26] ($P < 0.05$). GO and KEGG analyses not only bolster our hypothesis but also facilitate a comprehensive exploration of the precise locations of these genes within intricate biological networks, as well as their potential multifaceted roles. To delve deeper into the protein-level interactions among the candidate genes, a protein-protein interaction (PPI) network was constructed using the STRING database [27] (confidence scores > 0.4).

Single-cell data analysis

The GSE201048 dataset underwent preprocessing using the 'Seurat' package (version 4.3.0) [28]. Initially, cells were filtered based on quality criteria, retaining only those with a gene count ranging from 200 to 6000 and a mitochondrial gene proportion of less than 10%. Following this quality control (QC) step, the FindVariableFeatures function was utilized to select the top 2000 highly variable genes for subsequent analysis. Subsequently, a dimensionality reduction process was initiated. Initially, a normalization step was conducted using the global scaling method (LogNormalize). This involved normalizing the feature expression measurements in each cell by dividing by the total expression, multiplying the result by a scaling factor (default of 10 000), and then applying a log transformation to the normalized values. Secondly, following QC, the 'FindVariableFeatures' function was employed to identify the top 2000 highly variable genes. Principal component analysis was then conducted on these genes to obtain the optimal linear dimensions for cell clustering. Subsequently, the RunUMap function was utilized to classify the resulting cell clusters. Using the FindAllMarkers function from the R package 'Seurat', with parameters set tomin.pct = 0.1 and logfc.threshold = 0.5, differential gene expression analysis was conducted between different cell types. The selection criteria for marker genes were established as avg_$\log_2$ FC > 1 and p_val_adj <0.05. Based on the expression profiles of these marker genes, the cell clusters were annotated with specific cell types. Marker genes were obtained as previously described [13]. Annotation was

facilitated by the CellMarker website and 'SingleR' (version 2.0.0) [29,30].

Identification of key genes

Differential expression analysis was performed between various cell types using the FindMarkers function in 'Seurat' [$|\log_2$ fold-change (FC)| > 0.25, adj.$P < 0.05$], to identify significant differentially expressed genes (DEGs). Duplicate DEGs were subsequently removed for each cell type. Then, the candidate genes derived from the UVMR analysis were crossreferenced with the identified DEGs, and the overlapping genes were selected as key genes associated with epilepsy.

Localization of key genes on chromosomes and subcellular

The distribution of key genes across the human chromosome was visualized using Circos (https://circos.ca/) [31]. The subcellular locations of these key genes were then screened using the GeneCards (https://www.genecards.org/) database [32], with a confidence level >1 serving as the criterion. This analysis provides insights into the mechanisms by which these key genes are involved in epileptogenesis.

Functional similarity analysis between key genes and construction of a key gene interaction network.

The functional similarity among key genes was assessed using the 'GOSemSim' (version 2.18.1) [33]. Specifically, GO functional annotation data for the human species were obtained using appropriate Google functions. Based on this, the mgeneSim function was utilized to calculate the semantic similarity between them. Further, GO functional similarities among key genes employed to explore with the help of the 'GOSemSim' (version 2.18.1). GeneMANIA (https://www.genemania.org/) was utilized to identify other genes that share similar functions with the key genes.

Identification of key cells, as well as communication and functional analysis

The expression of key genes was analyzed across different cell types, and the cell types in which these genes were significantly expressed were designated as key cell types. To further investigate cellular communication, the 'CellChat' (version 1.6.1) [34] was utilized to analyze the number and strength of interactions between the key cell types via ligand-receptor interactions.

Analysis of the key cells heterogeneity

To investigate the heterogeneity of key cells, the expression profiles of these cells from GSE201048 were initially extracted. Subsequently, the key cells derived from epilepsy samples underwent two rounds of clustering to annotate them into distinct cellular subpopulations. The clustering results were visualized using RunUMAP, and for each subpopulation, the top three genes were selected for presentation based on $\log_2$ FC sorting. To gain insights into the functions and signaling pathways enriched in these key cells, ReactomeGSA (version 1.12.0) was employed for enrichment analysis.

Exploration of molecular regulatory mechanisms of key genes and potential targeted drugs

To investigate the molecular regulatory mechanisms of the key genes, an initial step involved predicting the miRNAs corresponding to these genes via 'multiMiR' (version 1.20.0) [35]. Subsequently, the upstream regulators of these miRNAs, namely lncRNAs, were predicted using the Star Base database [36]. By integrating the lncRNAs, miRNAs, and key genes, a competing endogenous RNAs (ceRNA) [37] network was constructed. To delve deeper into the regulatory relationships, a TF-mRNA-miRNA network was also established, incorporating transcription factors (TFs), key genes, and miRNAs. It is necessary to predict the potential TFs of key genes in the hTFtarget database [38]. Meanwhile, to identify potential drugs for the treatment of epilepsy, the 'enrichR' (version 3.2) [39] was used to predict drugs that act on key genes.

Statistical analysis

Bioinformatics analysis was performed through R software. Analyses were performed between these two groups using the Wilcoxon rank test. Differences were considered statistically significant at $P < 0.05$.

Results

There were 11 candidate genes significantly causally associated with epilepsy

MR analysis was conducted, with CCRs serving as the exposure factor and epilepsy as the outcome. Out of 64 CCRs analyzed, eleven were found to have a significant causal association with epilepsy and were identified as candidate genes. Among these,CCRL2, CCR2, CCL25, XCL2, CCL28, CXCL5, CXCL1, CX3CR1, and CCR3 emerged as risk factors for epilepsy (OR > 1, $P < 0.05$). Conversely, CXCR5 and CXCR1 were protective factors against epilepsy (OR < 1, $P < 0.05$) (Fig. 1a). The scatter plots illustrated that the IVW slope trends for CCRL2, CCR2, CCL25, XCL2, CCL28, CXCL5, CXCL1, CX3CR1, and CCR3 were positive, indicating that these exposure factors serve as risk factors for epilepsy. Conversely, the IVW slope trends for CXCR5 and CXCR1 were negative, reinforcing the notion that these exposure factors are protective against epilepsy (Fig. 2). This was subsequently confirmed through forest plots. The effect sizes for these nine exposure factors (CCRL2, CCR2, CCL25, XCL2, CCL28, CXCL5, CXCL1, CX3CR1, and CCR3) were all found to be greater than zero, indicating their role as risk factors for epilepsy. In contrast, the SNP loci for CXCR5 and CXCR1 were

Fig. 1

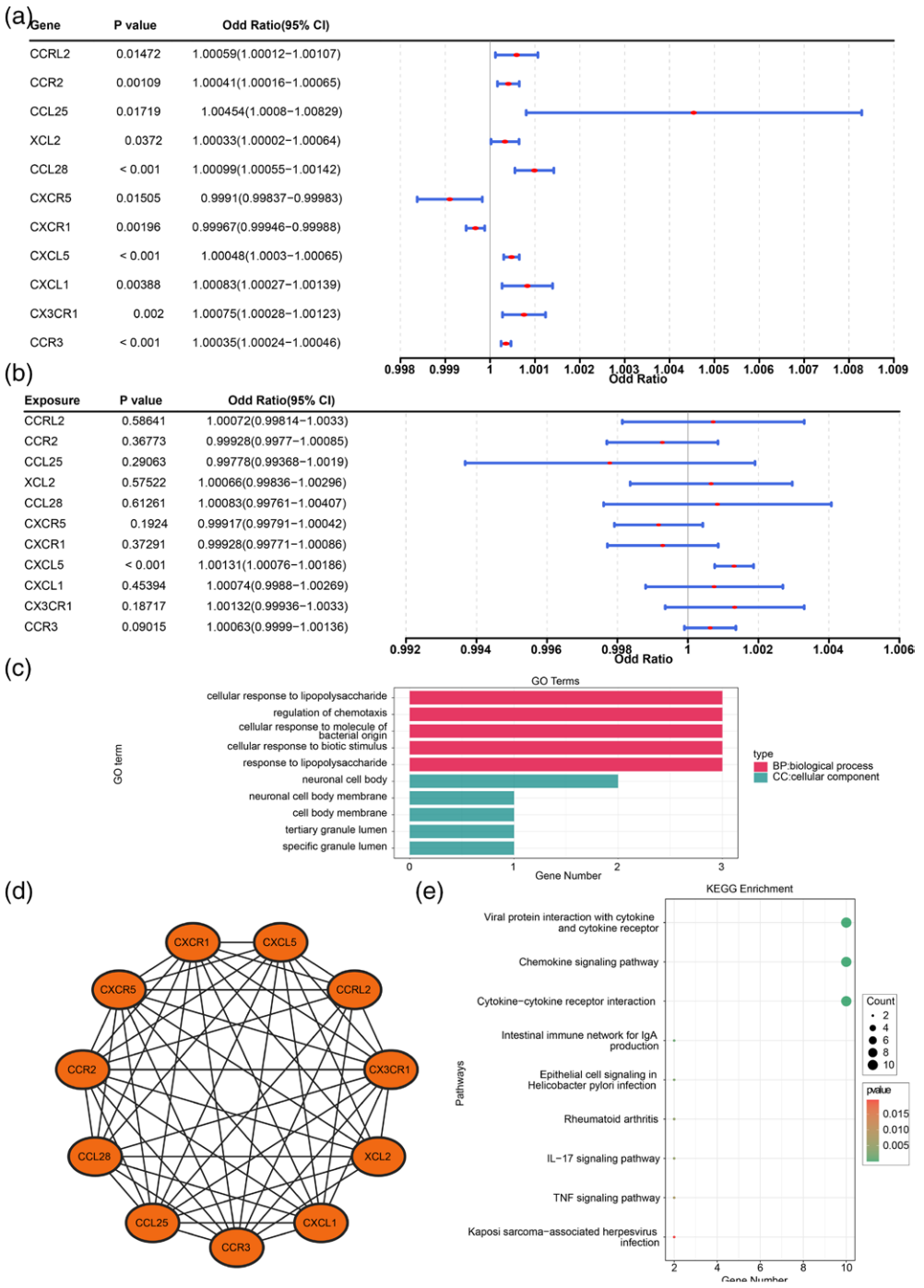

The MR and functional enrichment analysis of CCRs and epilepsy. (a) The results of UVMR analysis for candidate genes and epilepsy. (b) The results of MVMR analysis for candidate genes and epilepsy. (c) The results of GO enrichment analysis of candidate genes. GO entries on the horizontal axis and counts on the vertical axis indicate the number of genes enriched to either pathway; orange represents BP and blue represents CC. (d) The results of KEGG enrichment analysis of candidate genes. The horizontal coordinate was the number of genes enriched to any pathway, and the vertical axis was the KEGG pathway entry; the larger the circle, the greater the number of COUNTs; the greener the color represents a smaller, more significant *P*-value. (e) The PPI networks of candidate genes. The vibrant hue of orange is employed to denote the candidate genes, characterized by a local clustering coefficient of 0.953 and an enrichment *P*-value that falls below 1.0e−16. The connecting lines signify that the candidate genes engage in reciprocal interactions. BP, biological processe; CCRs, chemokine and chemokine receptor; GO, Gene Ontology; KEGG, Kyoto Encyclopedia of Genes and Genomes; MR, Mendelian randomization; MVMR, multivariable Mendelian randomization; PPI, protein-protein interaction; UVMR, Univariable Mendelian randomization.

Fig. 2

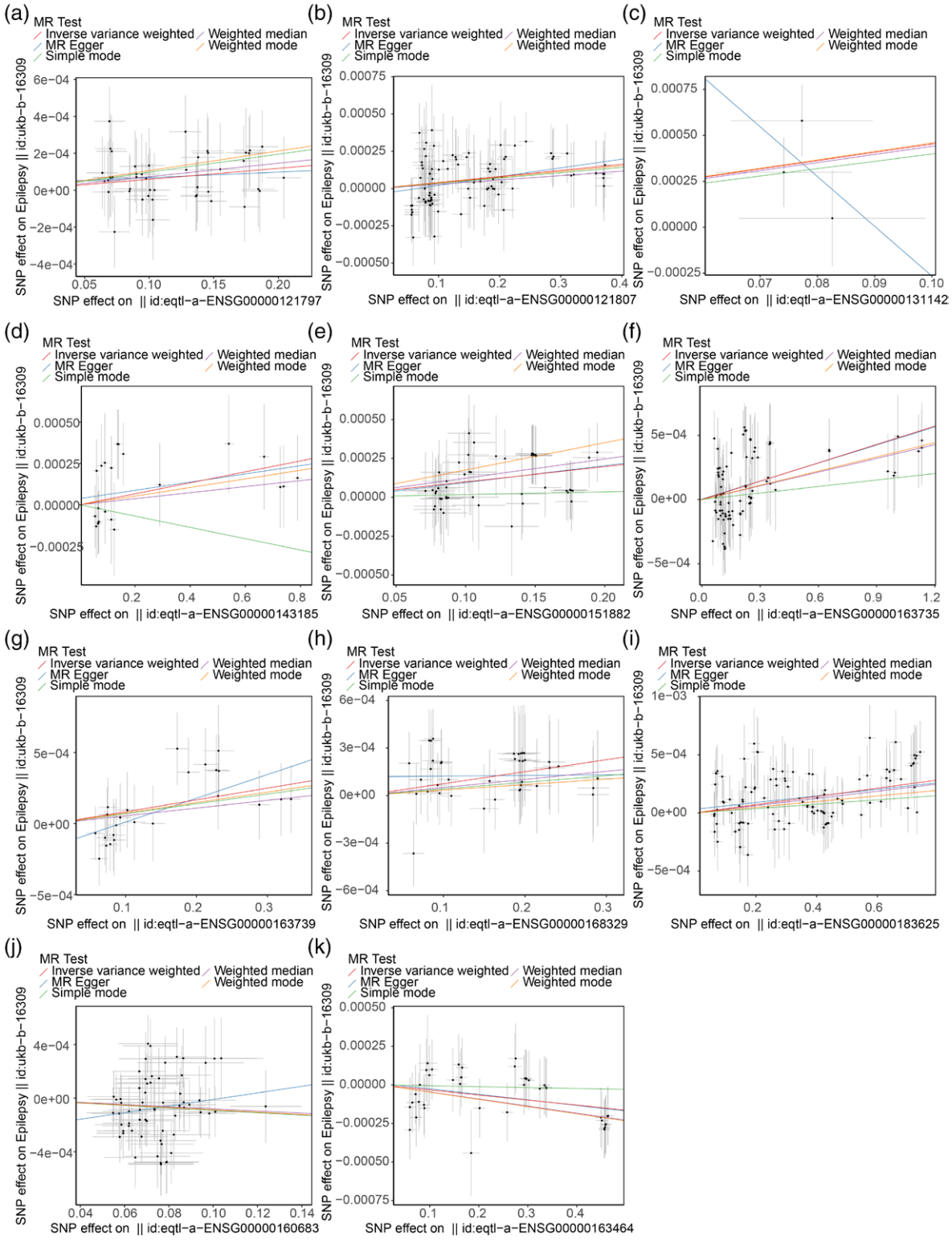

Scatter plots of UVMR analysis for candidate genes and epilepsy. (a) CCRL2. (b) CCR2. (c) CCL25. (d) XCL2. (e) CCL28. (f) CXCL5. (g) CXCL1. (h) CX3CR1. (i) CCR3. (j) CXCR5. (k) CXCR1. The horizontal coordinate was the effect of SNP on exposure, the vertical coordinate was the effect of SNP on outcome, and the colored lines indicate the results of fitting different algorithms for MR. A positive slope of the line indicates a risk factor and a negative slope of the line indicates a safety factor. When there was an intercept, the presence of confounding factors was implied. MR, Mendelian randomization; SNP, single nucleotide polymorphism; UVMR, Univariable Mendelian randomization.

Fig. 3

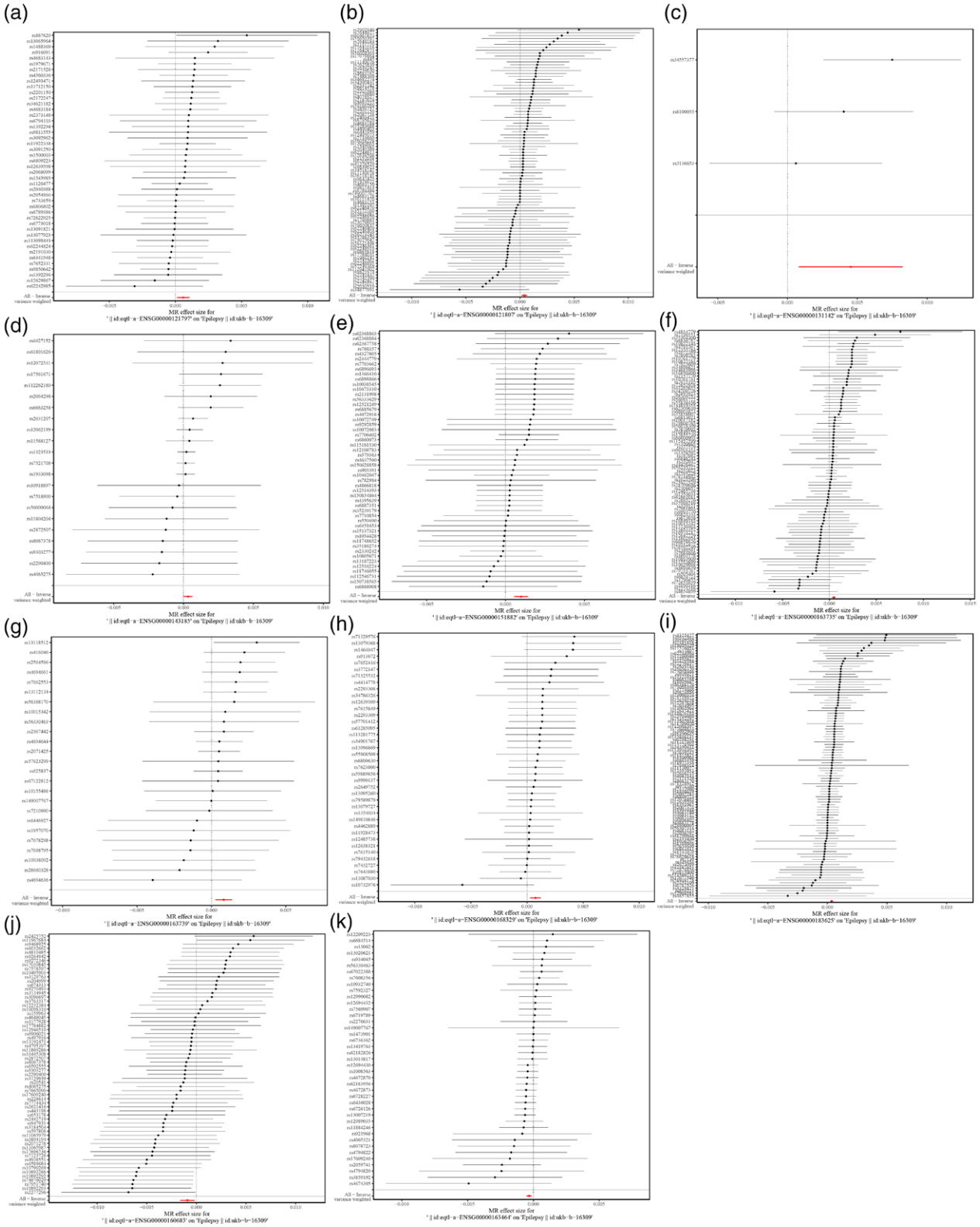

Forest plots of UVMR analysis for candidate genes and epilepsy. (a) CCRL2. (b) CCR2. (c) CCL25. (d) XCL2. (e) CCL28. (f) CXCL5. (g) CXCL1. (h) CX3CR1. (i) CCR3. (j) CXCR5. (k) CXCR1. Each horizontal solid line in the figure reflects the results of a single SNP estimated using the Wald ratio method, with the solid line entirely to the left of 0 indicating that the result estimated from this SNP was that an increase in exposure factors reduces the risk of the outcome variable, and the solid line entirely to the right of 0 indicating that the result estimated from this SNP was that an increase in exposure factors elevates the risk of the outcome variable. SNP, single nucleotide polymorphism; UVMR, Univariable Mendelian randomization.

Fig. 4

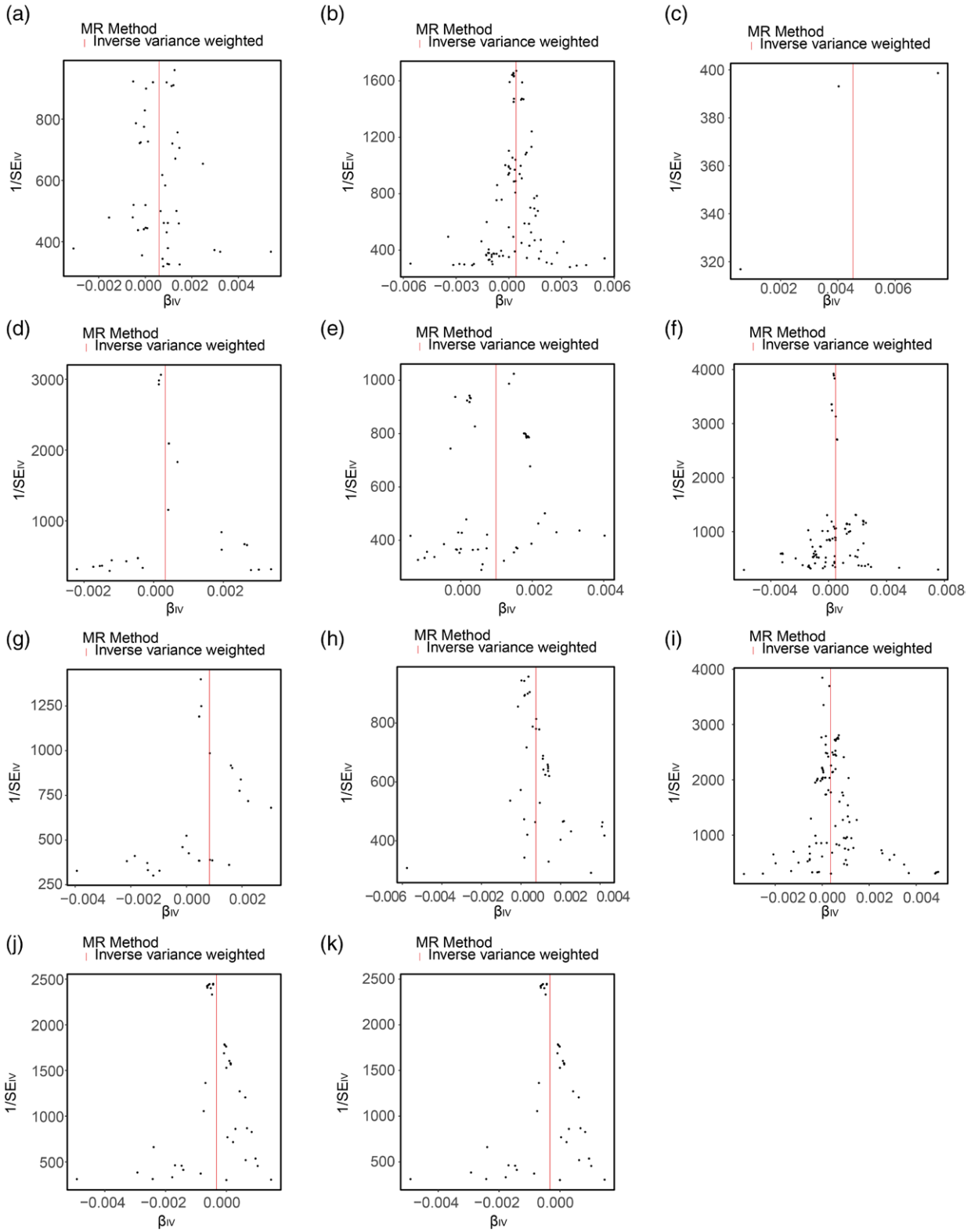

Funnel plots of UVMR analysis for candidate genes and epilepsy. (a) CCRL2. (b) CCR2. (c) CCL25. (d) XCL2. (e) CCL28. (f) CXCL5. (g) CXCL1. (h) CX3CR1. (i) CCR3. (j) CXCR5. (k) CXCR1.The horizontal axis of the graph was the β-value of the instrumental variable and the vertical axis was the inverse of the standard error of the instrumental variable. UVMR, Univariable Mendelian randomization.

Table 1 **The results of heterogeneity, horizontal pleiotropy, and Steiger test**

Heterogeneity test	Symbol	id.exposure	Method	*Q*	Q_df	Q_*P* value
	CCL25	eqtl-a-ENSG00000131142	IVW	2.98869072	2	0.224395455
	CCL28	eqtl-a-ENSG00000151882	IVW	19.06550285	50	0.999977957
	CCR2	eqtl-a-ENSG00000121807	IVW	39.75148475	89	0.999998627
	CCR3	eqtl-a-ENSG00000183625	IVW	68.13136745	100	0.993822821
	CCRL2	eqtl-a-ENSG00000121797	IVW	16.48615784	44	0.999948603
	CX3CR1	eqtl-a-ENSG00000168329	IVW	17.47950342	38	0.998234963
	CXCL1	eqtl-a-ENSG00000163739	IVW	13.92561299	24	0.948312637
	CXCL5	eqtl-a-ENSG00000163735	IVW	104.3415448	88	0.112677444
	CXCR1	eqtl-a-ENSG00000163464	IVW	18.70479358	40	0.998355986
	CXCR5	eqtl-a-ENSG00000160683	IVW	72.09018276	63	0.202533832
	XCL2	eqtl-a-ENSG00000143185	IVW	14.02163529	21	0.868668155
Horizontal pleiotropy test	Symbol	ENSEMBL	se	*P* value	Symbol	ENSEMBL
	CCRL2	eqtl-a-ENSG00000121797	8.91E-05	0.667414485	CCRL2	eqtl-a-ENSG00000121797
	CCR2	eqtl-a-ENSG00000121807	4.48E-05	0.405334376	CCR2	eqtl-a-ENSG00000121807
	CCL25	eqtl-a-ENSG00000131142	0.004434026	0.679683738	CCL25	eqtl-a-ENSG00000131142
	XCL2	eqtl-a-ENSG00000143185	6.12E-05	0.546553498	XCL2	eqtl-a-ENSG00000143185
	CCL28	eqtl-a-ENSG00000151882	0.000104686	0.894555261	CCL28	eqtl-a-ENSG00000151882
	CXCR5	eqtl-a-ENSG00000160683	0.000158011	0.109685533	CXCR5	eqtl-a-ENSG00000160683
	CXCR1	eqtl-a-ENSG00000163464	6.11E-05	0.866746283	CXCR1	eqtl-a-ENSG00000163464
	CXCL5	eqtl-a-ENSG00000163735	3.75E-05	0.925626742	CXCL5	eqtl-a-ENSG00000163735
	CXCL1	eqtl-a-ENSG00000163739	8.67E-05	0.084103718	CXCL1	eqtl-a-ENSG00000163739
	CX3CR1	eqtl-a-ENSG00000168329	8.86E-05	0.186716869	CX3CR1	eqtl-a-ENSG00000168329
	CCR3	eqtl-a-ENSG00000183625	4.38E-05	0.468754484	CCR3	eqtl-a-ENSG00000183625
Steiger test	SYMBOL	id.exposure	steiger_dir	steiger_pval	Symbol	id.exposure
	CCL25	eqtl-a-ENSG00000131142	TRUE	1.05×10^{-6}	CCL25	eqtl-a-ENSG00000131142
	CCL28	eqtl-a-ENSG00000151882	TRUE	2.78×10^{-31}	CCL28	eqtl-a-ENSG00000151882
	CCR2	eqtl-a-ENSG00000121807	TRUE	5.03×10^{-24}	CCR2	eqtl-a-ENSG00000121807
	CCR3	eqtl-a-ENSG00000183625	TRUE	3.97×10^{-7}	CCR3	eqtl-a-ENSG00000183625
	CCRL2	eqtl-a-ENSG00000121797	TRUE	1.11×10^{-47}	CCRL2	eqtl-a-ENSG00000121797
	CX3CR1	eqtl-a-ENSG00000168329	TRUE	2.08×10^{-5}	CX3CR1	eqtl-a-ENSG00000168329
	CXCL1	eqtl-a-ENSG00000163739	TRUE	4.18×10^{-9}	CXCL1	eqtl-a-ENSG00000163739
	CXCL5	eqtl-a-ENSG00000163735	TRUE	2.07×10^{-15}	CXCL5	eqtl-a-ENSG00000163735
	CXCR1	eqtl-a-ENSG00000163464	TRUE	0	CXCR1	eqtl-a-ENSG00000163464
	CXCR5	eqtl-a-ENSG00000160683	TRUE	7.51×10^{-12}	CXCR5	eqtl-a-ENSG00000160683
	XCL2	eqtl-a-ENSG00000143185	TRUE	1.07×10^{-7}	XCL2	eqtl-a-ENSG00000143185

positioned on the left side of the zero line, further reinforcing their status as protective factors against epilepsy (Fig. 3). SNPs were uniformly and randomly distributed on both sides of the IVW line, suggesting that the analyses followed Mendel's second law (Fig. 4). In addition, the *F*-statistic results showed that all SNPs had *F*-values > 20, indicating the absence of weak IVs.

In the heterogeneity test, all the *P*-values of the IVW statistics exceeded 0.05, suggesting the absence of heterogeneity between the exposure factor and epilepsy datasets (Table 1). Furthermore, in the horizontal pleiotropy test, the *P*-values for these exposure factors were also above 0.05, indicating that no horizontal multidimensionality was present in the analysis (Table 1). The causal relationship between these exposure factors and epilepsy did not change significantly after excluding one SNP, thus confirming the stability of the results (Supplementary Fig. 1, Supplemental Digital Content, *https://links.lww.com/WNR/A823*). Immediately following this, CXCR5 and CXCR1 remained protective factors against epilepsy in MVMR results. CCR2 and CCL25, which are risk factors in the UVMR results, were shown to be protective factors in the MVMR results (Fig. 1b). This suggested that there may be interactions between these genes. Finally, all 11 CCRs passed the Steiger test ($P < 0.0001$; the causal direction was true), confirming that the UVMR results were unaffected by reverse causation (Table 1). Based on these results, CCRL2, CCR2, CCL25, XCL2, CCL28, CXCL5, CXCL1, CX3CR1, CCR3, CXCR5, and CXCR1 were identified as potential candidate genes.

These 11 candidate genes were significantly enriched in chemokine signaling pathways

To delve into the biological roles and the underlying signaling pathways associated with the candidate genes, we conducted GO and KEGG enrichment analyses on 11 key genes, which were found to be associated with 217 GO biological functions. This encompassed 192 biological processes, 19 molecular functions, and six cellular components. The top five most prominently enriched entries include 'cellular chemotaxis, chemokine-modulated signaling pathways, chemokines, and neuronal cell bodies', all of which are linked to CCRs (Fig. 1c). KEGG analysis revealed that the implicated genes were predominantly concentrated in nine distinct signaling pathways, with the 'chemokine signaling pathway' showing a notable correlation with CCRs (Fig. 1d). The eleven candidate gene proteins were intricately interconnected within the PPI network, creating a sophisticated network akin to an intricate tapestry. This suggests that their collaborative interactions might function synergistically, with each protein pair collectively orchestrating the normal operation

of a distinct biological process (Fig. 1e). CCRL*2*, XCL*2*, CXCR5, CXCL1, and CX3CR1 interact with each other.

CCRL2, XCL2, CXCR5, CXCL1, and CX3CR1 were key genes screened for epilepsy

A series of meticulous single-cell analyses were conducted to delve into the gene expression patterns in epilepsy at the individual cell level, thereby affirming the diverse cellular origins of the analyzed cells and pinpointing the specific cell types present within the samples from epilepsy patients. The single-cell data underwent rigorous QC measures, resulting in the acquisition of 85 000 cells and *22* 950 genes (Supplementary Fig. *2*, Supplemental Digital Content, *https://links.lww.com/WNR/A823*). Six cell types were annotated based on marker genes, namely Microglia, T cells, NVUs, macrophages, oligodendrocytes, and B cells. The predominant cell type within the brain's immune defense is microglia, playing a crucial role in neuropathological research as the primary immune cells (Fig. 5a, b). Subsequently, 6395 DEGs were identified in these six cell types, and the top three $\log_2$ FC genes in the six cell types are shown in Supplementary Fig. 3, Supplemental Digital Content, *https://links.lww.com/WNR/A823*. Subsequently, a comprehensive analysis involving 11 candidate genes that intersected with 6395 DEGs was conducted, resulting in the identification of CCRL*2*, XCL*2*, CXCL1, CXCR5, and CX3CR1 as key genes associated with epilepsy (Fig. 5c, Supplementary Table 1, Supplemental Digital Content, *https://links.lww.com/WNR/A823*). To elucidate the differential expression patterns of key genes between the affected and control cohorts, we leveraged the single-cell dataset GSE190452, encompassing control samples, to affirm gene expression levels. Initially, a rigorous QC process was conducted on the single-cell dataset GSE190452, as depicted in Fig. 5d, to ensure the retrieval of cells of superior quality. Subsequently, these cells were annotated, and because the dataset pertained to astrocytes, they were annotated as astrocytes (Fig. 5e). Subsequently, we validated the expression profiles of key genes by comparing the epilepsy group with the control group within the single-cell dataset. Violin plots were generated to visualize intergroup differences, demonstrating that key genes exhibited significant differences ($P < 0.05$) between the groups (Fig. 5f).

There was a strong functional similarity between five key genes

To gain insight into the chromosomal positioning of key genes, the distribution of five key genes (CCRL*2*, XCL*2*, CXCR5, CXCL1, and CX3CR1) across the chromosomes has been mapped. The chromosomal localization data reveal that XCL*2* is predominantly situated on chromosome 1, while CX3CR1 and CCRL*2* are primarily found on chromosome 3. CXCL1 is chiefly located on chromosome 4, and CXCR5 predominantly resides on chromosome 11 (Supplementary Fig. 4, Supplemental Digital Content, *https://links.lww.com/WNR/A823*). Five genes pivotal for subcellular localization were identified, collectively occupying nine distinct subcellular sites and exhibiting colocalization at both the external cell membrane and the intracellular cytoplasmic membrane (Fig. 6a). This was further demonstrated by the functional similarity results for the key genes. CCRL*2*, XCL*2*, CXCR5, CXCL1, and CX3CR1 showed high average functional similarities (critical value > 0.5) (Fig. 6b). Twenty key genes were predicted to be functionally relevant (Fig. 6c). The key genes exhibited 150 functional interactions with these 20 genes, notably encompassing roles linked to CCRs such as 'cytokine activity', 'chemokine receptor binding', 'cellular responses to chemokines', and 'chemokine-mediated responses'.

Microglia, B cells, T cells, and macrophages were recognized as key cells, and they were involved in the body's inflammatory response

To identify the key cells, the expression of the five key genes (CCRL*2*, XCL*2*, CXCR5, CXCL1, and CX3CR1) was viewed in different cells in the single-cell dataset, and the cells in which all the key genes were significantly expressed were selected as the key cells. The key genes were most significantly expressed in microglia, B cells, T cells, and macrophages, and these four cells were identified as key cells (Fig. 7a–c). CCRL*2* was predominantly found in macrophages, with XCL*2* reaching its peak expression in T cells, CXCR5 exhibiting the highest levels in B cells, while CX3CR1 and CXCL1 were most prominently expressed in microglia.

Microglia were classified into 11 subpopulations, T cells into five subpopulations, B cells into five subpopulations, and macrophages into seven subpopulations (Fig. 7d). The diverse nature of pivotal cells indicates that chemokines could play a role in the molecular mechanisms underlying epilepsy. Moreover, the cellular communication findings revealed that microglia are the predominant cells and exhibit robust interactions with macrophages (Fig. 8a, b). In contrast, the ligand-receptor interactions between macrophages and microglia are quite abundant. Notably, within these interactions, the engagement between macrophages and microglia, as well as macrophages and oligodendrocytes, the SPP1-CD44 pairing stands out as the most robust (Fig. 8c). The results of the functional enrichment analysis of key cell clusters indicated that the common signaling pathways shared by Macrophages, T cells, B cells, and microglia encompass hydroxycarboxylic acid-binding receptors, which bind to repetitive carbohydrate structures on the target cell surface; COX reactions; acetylcholine inhibited contraction of outer hair cells; synthesis of epoxy (EET) and dihydroxyeicosatrienoic acids, histamine receptors, FGFR1c and Klotho ligand binding and activation, and proton-coupled neutral amino acid transporters (Fig. 8d).

Fig. 5

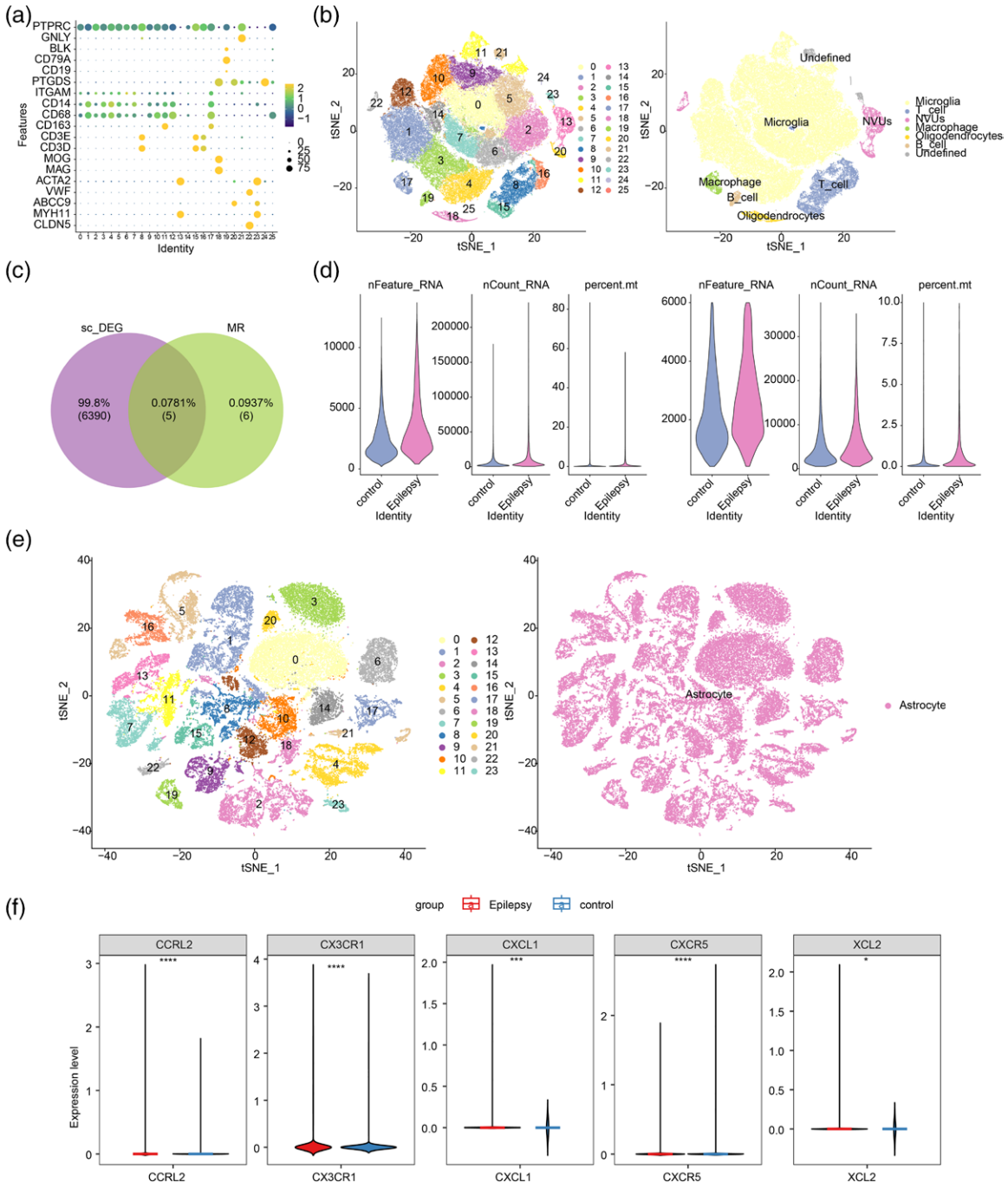

The identification of key genes. (a) Expression of marker genes in cell clusters. (b-1) UMAP cluster map of annotated cell types. (b-2) tSNE clustering map after cell annotation for different taxa. Different colors represent different taxa. The horizontal and vertical coordinates indicated the position of the data points in the low-dimensional space. Different colors represented different taxa. (c) Venn diagram of DEGs genes and candidate genes. (d-1) Differences in expression of key genes between disease and control before QC. (d-2) Differences in expression of key genes between disease and control after QC. The horizontal and vertical coordinates represented the cell type, the vertical coordinate in the nFeature_RNA plot represented the number of genes measured per cell, the vertical coordinate in the nCount_RNA plot represented the sum of the expression of all the genes measured per cell, and the vertical coordinate in the percent.mt plot represented the proportion of mitochondrial genes measured per cell. (e) Cellular annotation plot of cells after QC. Horizontal and vertical coordinates were TtSNE loci, different colors represented different taxa. (f) Expression of key genes was analyzed between Epilepsy disease and control controls. The horizontal coordinates represented the Epilepsy disease and control groups, with the Epilepsy disease group in red and the control group in blue. Vertical coordinates represented expression. $^{*}P < 0.05$; $^{***}P < 0.001$; and $^{****}P < 0.0001$. DEGs, differentially expressed genes; QC, quality control; UMAP, Univariable Mendelian randomization.

Fig. 6

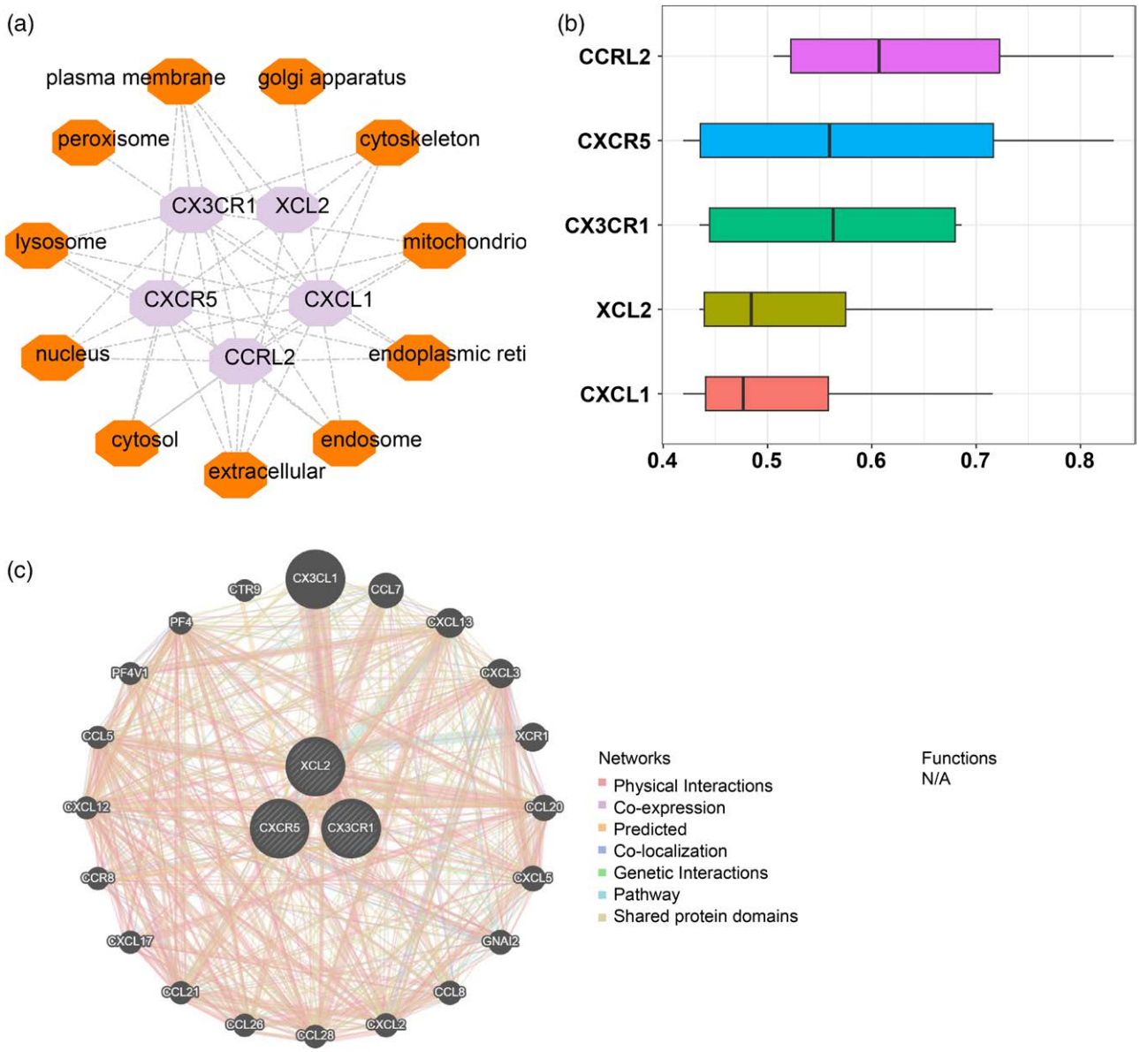

The localization and functional similarity of key genes. (a) Subcellular localization of key genes. Pink for key genes, orange for subcellular loci. (b) The results of functional similarity analysis of key genes. Horizontal coordinates were similarity scores and vertical coordinates were key genes. (c) The top 20 genes associated with key gene functions.

Totally 27 drugs were more effective for epilepsy patients

To delve into the molecular regulatory processes governing the five key genes (CCRL2, XCL2, CXCR5, CXCL1, and CX3CR1), miRNAs and TFs of key genes were predicted, and miRNAs acted as hub miRNAs connecting the key genes and lncRNAs. Furthermore, a TF regulatory network and a drug prediction network focusing on key genes have been meticulously constructed. In the ceRNA network, only CXCL1 predicted the complete lncRNA-miRNA-mRNA regulatory network (Supplementary Fig. 5a, Supplemental Digital Content, *https://links.lww.com/WNR/A823*). CXCL1 is the sole predictor of the lncRNA-miRNA-mRNA regulatory cascade. This complex regulatory framework entails the fine-tuning of CXCL1 through the action of two distinct miRNAs: hsa-miR-570-3p and hsa-miR-532-5p. The regulation of CX3CR1 is governed by a set of three miRNAs, which include hsa-miR-644a, hsa-miR-1227-3p, and hsa-miR-4261. In the TF regulatory network, CCRL2 was predicted to interact with 37 TFs, whereas CX3CR1 was predicted to interact with nine TFs. No corresponding TFs were predicted for the other genes

Fig. 7

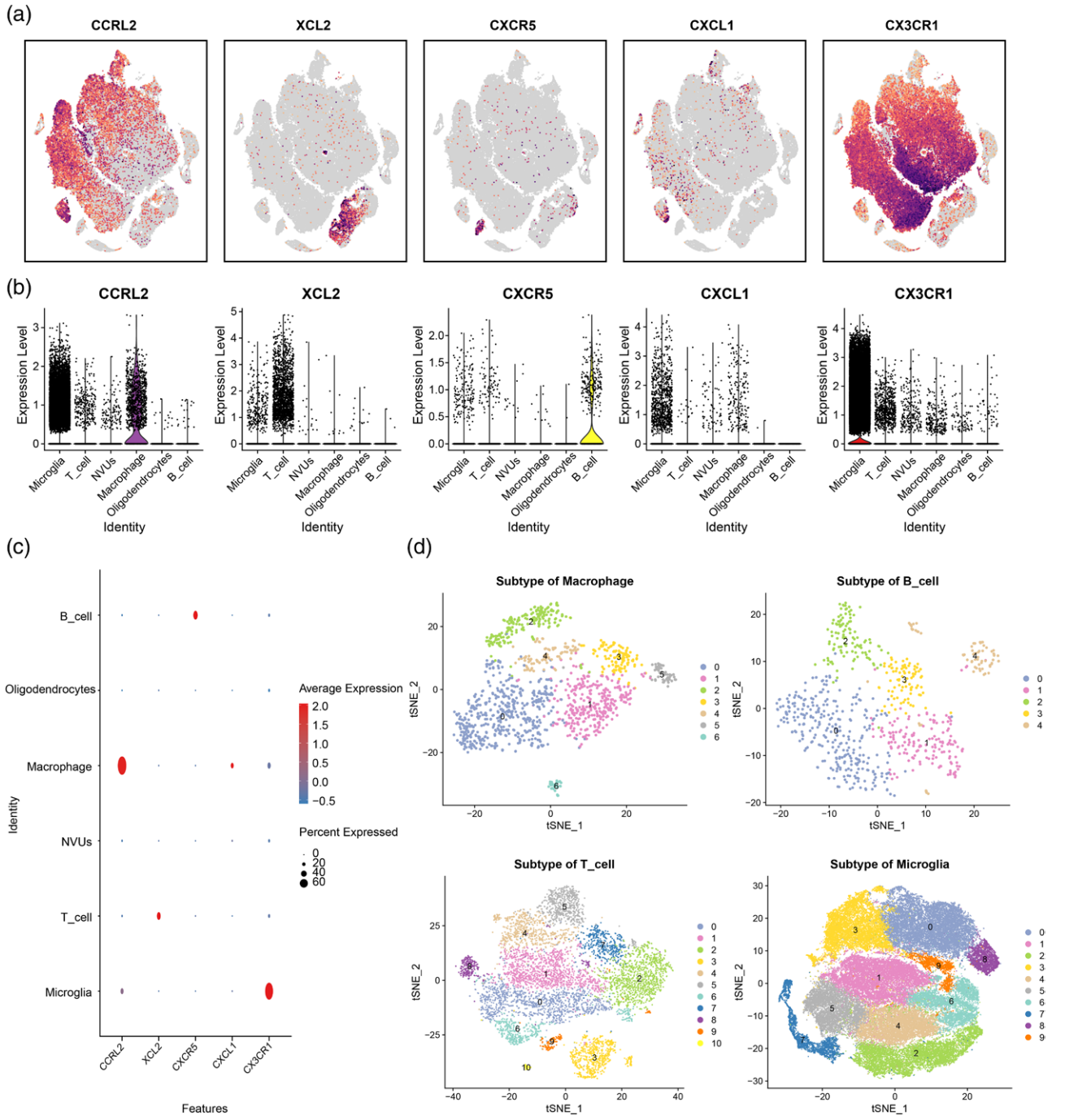

Annotation of key cell subpopulations. (a) Expression of key genes in different cells. (b) Violin plots of the expression of key genes in different cells. Horizontal coordinates represented key cell types and vertical coordinates represented the amount of expression. (c) Expression of key genes in 6 cell subpopulations. (d-1) Annotation of 7 subpopulations of macrophages. (d-2) Annotation of 5 subpopulations of B cells. (d-3) Annotation of 11 subpopulations of T cells. (d-4) Annotation of 11 subpopulations of Microglia. The horizontal and vertical coordinates represented the position of tSNE.

(Supplementary Fig. 5b, Supplemental Digital Content, *https://links.lww.com/WNR/A823*). Moreover, the analysis of drug predictions linked to key genes revealed that CXCR5 is associated with 21 pharmacological agents, CXCL1 with 4, CX3CR1 with 2, while no pertinent drug compounds were forecasted for the rest of the genes (Supplementary Fig. 5c, Supplemental Digital Content, *https://links.lww.com/WNR/A823*).

Fig. 8

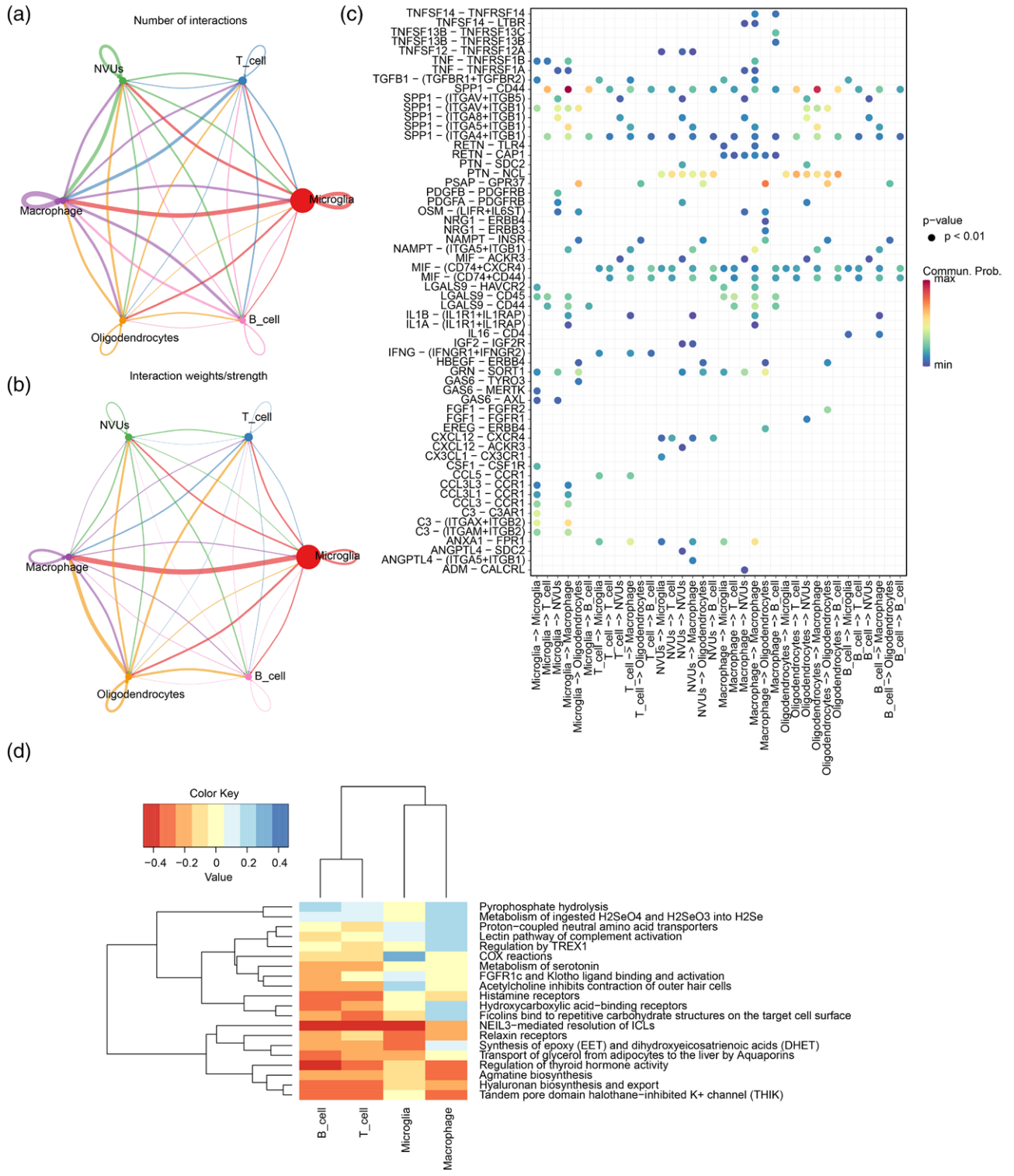

Functional enrichment of key cells. (a) Number of interactions in key cells. The size of the various colored circles around the periphery indicates the number of cells; the larger the circle, the greater the number of cells. Cells that emit arrows express ligands, and cells to which the arrows point express receptors. The more ligand-receptor pairs there are, the thicker the line. (b) Interaction weights/strength in key cells. (c) Ligand-receptor interactions for key cell communication. Arrows emanating from the horizontal coordinates were cells expressing ligands, and cells pointed to by arrows express receptors. The colors represent the intensity of the action. (d) The results of functional enrichment of key cell subsets. The horizontal axis showed the different subpopulations and the vertical axis showed the enrichment pathways. Each row was a pathway and each column was a subpopulation.

Discussion

Chemotactic agents not only elicit the migration of peripheral leukocytes into the central nervous system (CNS) across the blood-brain barrier, leading to their accumulation in sites of injury, but recent investigations also indicate their role in modulating voltage-gated ion channels and exerting immunomodulatory influences [40]. It has been found that the expression of CX3CL1, CCR5, CCL*2*, and CCR*2* are upregulated in the brain tissue of patients with epilepsy [41–43]. In particular, CX3CL1, through the phosphorylation of individual or multiple components of GABAA, diminishes the excitability of neurons affected by epilepsy, which in turn results in an elevated expression of CX3CL1 within the brain tissue of those suffering from TLE [36]. Furthermore, the expression of CCR5 and its corresponding ligands, CCL3 and CCL5, is increased in the hippocampal tissues of epilepsy patients and epilepsy rat models, accompanied by an increase in CCR5-positive [42,43].

This study confirmed that CCRL*2*, XCL*2*, CXCR5, CXCL1, and CX3CR1 are the key genes involved in epilepsy. XCL*2* (X–C motif chemokine ligand) is a small member of the X–C family of chemokines and is closely linked to other chemokines. In several cancers, including melanoma, nonsmall cell lung cancer, prostate cancer, and colorectal cancer, high levels of XCL*2* expression have been reported [44]. Kamimura *et al.* identified overexpression of XCL*2* in lung cancer and its association with disease prognosis [45]. The elevated levels of XCL*2* in the peripheral blood of individuals suffering from chronic neuropathic pain indicate a potential intimate association between XCL*2* and the progression of both chronic neuropathic pain and various forms of cancer [46]. XCL*2* is integral to the immune response, stimulating the activation of cytotoxic T cells. Advanced transcriptomic and single-cell sequencing analyses have elucidated that XCL*2* is intimately associated with the functions of T lymphocytes and macrophages, thereby highlighting its pivotal role within the immune system. Furthermore, XCL*2*, a pivotal chemokine across various cancers, presents novel potential therapeutic targets and treatment approaches for cancer management [47]. In the cerebral tissue specimens of epilepsy patients, we observed a notable association between the expression levels of XCL*2* and the recurrence rate of epileptic episodes. This correlation is particularly intriguing given that epileptic seizures have the potential to elicit atypical immune reactions within the brain [48,49]. It is speculated that XCL*2* may be involved in epilepsy-related immune responses by being attracted to lymphocytes into brain tissue. In essence, XCL*2* appears to be a pivotal factor in both chronic neuropathic pain and across diverse forms of cancer. Nonetheless, the intricacies of its role in epilepsy remain underexplored, necessitating additional research to unravel its functional underpinnings.

The exclusive receptor for CXCL13, designated as CXCR5 (C-X-C chemokine receptor type), was once referred to as the Burkitt lymphoma receptor 1. Nonetheless, studies have indicated that animals lacking CXCL13 exhibit normal migration of B cells within the CNS, albeit with a moderate and self-resolving instance of experimental autoimmune encephalomyelitis (EAE) [50], suggesting that CXCL13/CXCR5 in the CNS may regulate this neuroinflammatory disease. Recently, there has been a greater focus on the role of CXCR5 in brain development [51,52]. Studies have uncovered that CXCR5 plays a pivotal role in the regulation of neural stem cells, neuronal differentiation [53,54], neurogenesis, gliogenesis, and synaptogenesis [10,55] in the mouse brain. Further, a lack of CXCR5 during embryonic development leads to abnormal neuronal polarity, impaired neuronal migration, and increased neuronal hyperexcitability, ultimately resulting in increased vulnerability to epileptic seizures and convulsions [10]. Following the induction of status epilepticus (SE) in a pilocarpine-induced rat model, the protein concentrations of CXCL13 and CXCR5 underwent modifications across the varying phases of epilepsy [50]. Furthermore, dual-label immunofluorescence examination revealed that CXCL13 was predominantly localized within the membranes and cytoplasm of neurons and astrocytes, whereas CXCR5 was primarily detected in the membranes and cytoplasm of neuronal cells. This suggests that the CXCL13-CXCR5 pathway may play a pathogenic role in intractable epilepsy [50]. In the wake of epileptic seizures, the inflammatory response may lead to an abnormal attraction of B lymphocytes to the brain tissue, facilitated by the CXCR5–CXCL13 axis, subsequently impacting the immunological equilibrium within the brain. These B lymphocytes could be implicated in the synthesis of autoantibodies or the secretion of inflammatory mediators, which consequently lead to neuronal harm and are linked to the pathophysiology of epilepsy [56]. The precise mechanism by which CXCR5 exerts its regulatory influence on epilepsy continues to elude us, necessitating additional exploration and in-depth study.

Recently, these SNPs have emerged as pivotal disease-modifying factors in the realm of neurodegenerative disorders. Notably, the loss-of-function variants of the microglial fractalkine receptor, CX3CR1, have been linked to heightened Braak staging in Alzheimer's disease, expedited neurodegenerative processes, and a diminished survival rate in patients with amyotrophic lateral sclerosis [57–59]. One of the several important neuroglial communication axes that maintain microglial homeostasis is signaling via CX3CR1 and its neuronal ligand CX3CL1 [59,60]. CX3CR1-signaling not only actively dampens microglial phagocytosis and neurotoxic/pro-inflammatory activation during healthy aging but also inhibits NMDA- and glutamate-dependent Ca^{2+} influx into neurons, thereby protecting against neuronal excitotoxicity [7,61]. Indeed, the disruption of CX3CR1

amplifies inflammatory signaling within microglial cells, a phenomenon that corresponds with an exacerbated loss of dopaminergic neurons in the substantia nigra, as observed in murine models of Parkinson's disease [61,62]. The FKN/CX3CR1 pathway contributes to migraine-like symptoms by triggering the activation of microglia in the thalamic-cortical network of rats experiencing SE [63]. In summary, abnormal CX3CR1 function may lead to abnormal activation of macrophages in the brain tissue, releasing excessive inflammatory mediators. Especially the signaling of particular, which is associated with the pathological process of epilepsy [64]. CX3CL1, a key signaling molecule, plays a central role in the interaction between microglia and neurons. It not only finely regulates the basic physiological activities of the nervous system during development, adulthood, and aging but also enhances the survival of neurons and their precursor cells and regulates synaptic transmission and plasticity [65]. The disruption in CX3CL1 signaling is intimately linked with a myriad of neuropathological disorders, with its expression being susceptible to the impacts of external toxic agents. This molecule demonstrates an intricate interplay of both stimulatory and inhibitory influences in the context of diseases such as multiple sclerosis, inflammation triggered by EAE, epilepsy, and brain neoplasms, thereby underscoring the Janus-like role of CX3CL1 in the maintenance of neurological wellness and the onset of diseases [66].

CXCL1, a pivotal chemokine, serves as a critical cytokine in modulating the course of diverse inflammatory disorders, predominantly through the activation of CXCR2 and CXCR1. Its expression is significantly upregulated in the inflammatory response, which profoundly affects the pathological process and plays a key role in inducing angiogenesis and promoting neutrophil recruitment at the physiological level [67]. The C-X-C chemokine ligand (CXCL) 1, alongside its corresponding receptor CXCR2, is extensively distributed throughout both the peripheral nervous system and the CNS. They don't just engage in the inflammatory response and the regulation of pain following nerve damage, but also significantly impact the direct harm to neurons and the resultant secondary injuries within their primary regions. Activation of the CXCL1/CXCR2 axis can trigger injury-related pathways in neurons, whereas the expression of CXCR2 in astrocytes promotes cell proliferation but weakens its function and jointly and complexly regulates pathophysiological processes after nerve injury [68]. CCRL2 stands out as a distinctive chemokine receptor featuring seven transmembrane domains. Despite exhibiting a structural analogy to the unconventional chemokine receptor, it lacks both the chemotactic capabilities and the functions associated with clearing chemokines. It selectively adheres to the chemokine chemerin and is found within both leukocytes and nonhematopoietic cellular structures. Gene ablation studies, CCRL2 have revealed that it plays a key role in the regulation of inflammation, but its specific role as a positive or negative regulatory factor requires further exploration [69]. It was found that CCRL2 might be associated with an inflammatory response following epileptic seizures. Seizures are often accompanied by inflammatory reactions in the brain, and the expression level of CCRL2 in the brain undergoes significant changes after seizures [70]. It was speculated that CCRL2 may affect the inflammatory microenvironment following epileptic seizures by being involved in regulating the distribution and activity of inflammatory cells in the brain.

This investigation pinpointed T cells, B cells, microglia, and macrophages as pivotal CCs, with a quintet of key genes—CCRL2, XCL2, CXCR5, CXCL1, and CX3CR1—exhibiting differential expression levels across these distinct cell types. Communication analysis revealed a strong interaction between macrophages and microglia, suggesting that stimulating these cells may promote epilepsy development by increasing the expression of CCRL2, XCL2, CXCR5, CXCL1, and CX3CR1. Conversely, inhibition of these cell interactions could potentially improve epilepsy conditions. Ligand-receptor interactions between macrophages and B cells have been identified, with pairs such as SPP1-(ITGAV+ITGB1), TNF-TNFRSF1B, and LGALS9-CD44, which are potential therapeutic targets for epilepsy [71]. SPP1 is implicated in the modulation of host immune responses, with earlier research indicating that it can adeptly regulate the immune system of the host by enhancing the expression of IL-12 and IFNγ within murine macrophages and natural killer cells [72,73]. SPP1 is upregulated in human glioma-associated macrophages [74]. SPP1 may affect the excitability of hippocampal neurons. A pivotal discovery for a prospective therapeutic approach aimed at modifying hippocampal functionality in a live setting is the revelation that the impact is predominantly reliant on M1 receptor activity [75]. LGALS9 regulates the immune response and may affect epilepsy through immune cells and signaling [76–78]. Integrin subunit alpha V (ITGAV) is associated with KRAS signaling and immune activation [79]. The tumor necrosis factor receptor superfamily (TNFRSF), upon engaging with a diverse array of cytokines, exhibits an elevation in TNFRSF1B expression particularly within the context of Inflammatory Bowel Disease, thereby exacerbating the inflammatory reaction [80,81]. Animal models and human studies alike have demonstrated that the onset of epilepsy is significantly influenced by immune activation and the resultant inflammatory processes [82,83]. Anti-inflammatory therapy has been shown to be effective in controlling epileptic seizures [84]. Therefore, SPP1, TNFRSF, and LGALS9 regulate epilepsy through the inflammatory and immune pathways, including chemokines. In this investigation, the pathways consistently associated with the enhancement of macrophage and microglial populations were

identified as 'proton-coupled neutral amino acid transporters' and 'COX-mediated responses'. COX-2 serves as a pivotal target for therapeutic agents aimed at alleviating inflammation and pain. Although the interplay between genetic modification and pharmacological suppression of COX-2 has been investigated in the context of seizure disorders, the impact of COX-2 inhibitors on the onset of acute seizures has yielded variable outcomes within rodent experimental frameworks [85]. Recent evidence indicates that the underlying mechanism of epileptogenesis encompasses the interplay between adaptive and innate immune responses. Cytotoxic T cells and antibody-mediated complement activation are major components of the adaptive immune system that are capable of inducing neurodegeneration and are thought to contribute to epileptic encephalitis [86]. Furthermore, the administration of celecoxib, which inhibits COX-2, has been observed to mitigate cognitive deficits in epileptic mice induced by PTZ, indicating that cognitive impairments in these mice may be linked to neuroinflammation and neuronal damage caused by the COX-2-PGE2 pathway [87]. The biosynthesis of protection and catabolite coupling in tissue regeneration is closely related to neural metabolism [88]. Proton-coupled amino acid transporters, classified as SLC36As and commonly referred to as PAT, are integral members of the transmembrane amino acid cotransporter family. They exhibit distinct expression profiles and display a range of substrate specificities [89]. Currently, there is no research on whether it is involved in the development of epilepsy, apart from its function as an AA transporter protein [90,91]. These pathways are integral to the development of CNS disorders, such as epilepsy, though the precise molecular mechanisms at play have yet to be fully elucidated.

Currently, despite the presence of potentially impactful components or structures within compounds like digeranyl bisphosphonate, BPH-742, COMPOUND 51, MINORONIC ACID, and WWL123 that could influence the epileptic process, there exists no definitive scientific proof to indicate their direct application in epilepsy treatment or to confirm their distinct antiepileptic properties. These compounds may affect epilepsy by regulating neurotransmitters, ion channels, neuroinflammation, and oxidative stress mechanisms; for example, digeranyl bisphosphonate was predicted through CXCL15, which is an effective inhibitor of geranyl pyrophosphate (GGPP) synthase [92]. It prevents protein geranylation by inhibiting GGPP synthase and thus affects intracellular signaling pathways [92]. Research has shown that inhibiting the biosynthesis of geranyl diphosphate synthase affects endocrine differentiation [93]. Research indicates that inhibitors of ABHD6 modulate the production of activity-dependent 2-arachidonoyl glycerol (2-AG), thereby triggering the activation of cannabinoid receptor 1, a feature observed in certain epileptic conditions [94]. Inhibition of ABHD6 by WWL-123 significantly reduces the frequency of chemically and genetically induced seizures in mice [94]. Hence, this medication holds promise as a viable therapeutic target for investigating the etiology and intervention approaches of disorders linked to abnormal endocrine differentiation. Nevertheless, the precise implications necessitate additional empirical investigation and clinical verification. This study revealed that CXCL1 is governed by hsa-miR-570-3p and hsa-miR-532-5p. Previous research has found that miR-570-3p is involved in the occurrence and development of breast cancer, osteosarcoma, and bladder cancer [95–97]; miR-570-3p overexpression can alleviate endothelial inflammatory injury in diabetes by mediating HDAC1 [98]. miR-532-5p exerts neuroprotective effects against ischemic stroke by suppressing PTEN expression and directly binding to CXCL1, consequently activating the PI3K/Akt signaling cascade, and holds potential as a novel therapeutic candidate for the treatment of ischemic stroke [99,100]. However, hsa-miR-570-3p and hsa-miR-532-5p have not been studied in epilepsy. In the inflammatory response of the brain after epileptic seizures, the expression of CXCL1 is significantly upregulated. It is believed that CXCL1 may exacerbate the inflammatory response in the brain by attracting a large number of neutrophils into brain tissue. Excessive aggregation of neutrophils in the brain tissue can release reactive oxygen species and proteases, causing direct damage to neurons and potentially disrupting the integrity of the blood-brain barrier, further exacerbating pathological changes after epileptic seizures [101].

This investigation was not without its limitations. Foremost, the compact sample size may have inadvertently introduced sampling bias, and as such, it failed to capture the complete range of genetic variations and clinical presentations associated with epilepsy, thus constraining the broad applicability and the representative nature of the findings. Secondly, in the course of performing cell RNA sequencing data analysis and MR, there are inherent subjective inaccuracies in the annotation of cell types and the quantification of gene expression, along with potential biases from certain confounding elements. Moreover, the genes that have been identified still require functional substantiation. Lastly, the findings of this study are grounded in data from European populations, which may exhibit genetic and environmental discrepancies when compared to other racial and regional groups. Consequently, the subsequent research endeavors could be enhanced by adopting the following strategies. Initially, assemble an extensive array of epilepsy patient samples from varied geographical locations and ethnic backgrounds to bolster the diversity and representativeness of the sample population. Second, combine multiple omics technologies, such as proteomics and metabolomics, the genetic and environmental confounding can be overcome, and the pathogenesis of epilepsy can be comprehensively explored. Additionally, the

specific roles and regulatory mechanisms of key genes in the occurrence and development of epilepsy can be clarified through methods such as gene editing techniques, cell experiments, animal models, and others. Finally, similar studies will be conducted among multiethnic and cross-regional populations to verify the generalizability of the results, explore specific differences, and assist in the personalized diagnosis and treatment of epilepsy.

In summary, the present investigation integrated scRNA-seq with GWAS findings to delve into the CCR-associated genes and their roles in the context of epilepsy. Our analysis highlighted CCRL2, XCL2, CXCR5, CXCL1, and CX3CR1 as key genes linked to epilepsy. Furthermore, our research revealed that microglia, B lymphocytes, T lymphocytes, and macrophages are integral to the onset and progression of epilepsy. The findings imply that modulating the expression of these genes and controlling the function of these immune cells could potentially mitigate the emergence and advancement of epilepsy. Nevertheless, additional validation is necessary to elucidate the precise regulatory mechanisms pertaining to chemokines and immune cells in the context of epilepsy.

Acknowledgements

This work was supported by the Nature Science Foundation of China under Grants (no. 82060252 and 81960350), Yunnan Basic Research Projects under Grant (no. 2018FB115), and Yunnan Health Training Project of High-level Talents under Grant (no. D-2024038), Union Foundation of Yunnan Provincial Science and Technology Department and Kunming Medical University of China under Grant (no. 202201AY070001-091), 535 Talent project of the First Affiliated Hospital of Kunming Medical University under Grant (no.202535Q05), Yunnan Revitalization Talent Support Program Grant (nos. XDYC-QNRC-2022-0328), and Basic Research Project of the Science and Technology Department of Yunnan Province (no, 202101AT070148).

All data generated in this study are included in this manuscript.

Conflicts of interest

There are no conflicts of interest.

References

1 Scheffer IE, Berkovic S, Capovilla G, Connolly MB, French J, Guilhoto L, *et al*. ILAE classification of the epilepsies: position paper of the ILAE Commission for Classification and Terminology. *Epilepsia* 2017; **58**:512–521.
2 Griss J, Viteri G, Sidiropoulos K, Nguyen V, Fabregat A, Hermjakob H. ReactomeGSA - efficient multi-omics comparative pathway analysis. *Mol Cell Proteomics* 2020; **19**:2115–2125.
3 Englot DJ, Morgan VL, Chang C. Impaired vigilance networks in temporal lobe epilepsy: mechanisms and clinical implications. *Epilepsia* 2020; **61**:189–202.
4 Gao H, Li J, Li Q, Lin Y. Identification of hub genes significantly linked to subarachnoid hemorrhage and epilepsy via bioinformatics analysis. *Front Neurol* 2023; **14**:1061860.
5 Zhu Y, Huang D, Zhao Z, Lu C. Bioinformatic analysis identifies potential key genes of epilepsy. *PLoS One* 2021; **16**:e0254326.
6 Kanner AM, Bicchi MM. Antiseizure medications for adults with epilepsy: a review. *JAMA* 2022; **327**:1269–1281.
7 Thijs RD, Surges R, O'Brien TJ, Sander JW. Epilepsy in adults. *Lancet* 2019; **393**:689–701.
8 Hughes CE, Nibbs RJB. A guide to chemokines and their receptors. *FEBS J* 2018; **285**:2944–2971.
9 Choi J, Selmi C, Leung PS, Kenny TP, Roskams T, Gershwin ME. Chemokine and chemokine receptors in autoimmunity: the case of primary biliary cholangitis. *Expert Rev Clin Immunol* 2016; **12**:661–672.
10 Zhang Z, Zhang H, Antonic-Baker A, Kwan P, Yan Y, Ma Y. CXCR5 Regulates Neuronal Polarity Development and Migration in the Embryonic Stage via F-Actin Homeostasis and Results in Epilepsy-Related Behavior. *Neurosci Bull* 2023; **39**:1605–1622.
11 Zhang Z, Li Y, Jiang S, Shi FD, Shi K, Jin WN. Targeting CCL5 signaling attenuates neuroinflammation after seizure. *CNS Neurosci Ther* 2023; **29**:317–330.
12 Hu Y, Gaedcke J, Emons G, Beissbarth T, Grade M, Jo P, *et al*. Colorectal cancer susceptibility loci as predictive markers of rectal cancer prognosis after surgery. *Genes Chromosomes Cancer* 2018; **57**:140–149.
13 Kumar P, Lim A, Hazirah SN, Chua CJH, Ngoh A, Poh SL, *et al*. Single-cell transcriptomics and surface epitope detection in human brain epileptic lesions identifies pro-inflammatory signaling. *Nat Neurosci* 2022; **25**:956–966.
14 Liang X, Yu G, Zha L, Guo X, Cheng A, Qin C, *et al*. Identification and comprehensive prognostic analysis of a novel chemokine-related lncRNA signature and immune landscape in gastric cancer. *Front Cell Dev Biol* 2021; **9**:797341.
15 Hemani G, Tilling K, Davey Smith G. Orienting the causal relationship between imprecisely measured traits using GWAS summary data. *PLoS Genet* 2017; **13**:e1007081.
16 Burgess S, Scott RA, Timpson NJ, Davey Smith G, Thompson SG; EPIC- InterAct Consortium. EPIC- InterAct Consortium: Thompson, using published data in Mendelian randomization: a blueprint for efficient identification of causal risk factors. *Eur J Epidemiol* 2015; **30**:543–552.
17 Bowden J, Davey Smith G, Haycock PC, Burgess S. Consistent estimation in Mendelian randomization with some invalid instruments using a weighted median estimator. *Genet Epidemiol* 2016; **40**:304–314.
18 Bowden J, Davey Smith G, Burgess S. Mendelian randomization with invalid instruments: effect estimation and bias detection through Egger regression. *Int J Epidemiol* 2015; **44**:512–525.
19 Hemani G, Zheng J, Elsworth B, Wade KH, Haberland V, Baird D, *et al*. The MR-base platform supports systematic causal inference across the human phenome. *Elife* 2018; **7**:e34408.
20 Hartwig FP, Davey Smith G, Bowden J. Robust inference in summary data Mendelian randomization via the zero modal pleiotropy assumption. *Int J Epidemiol* 2017; **46**:1985–1998.
21 Wu T, Hu E, Xu S, Chen M, Guo P, Dai Z, *et al*. clusterProfiler 4.0: a universal enrichment tool for interpreting omics data. *Innovation (Camb)* 2021; **2**:100141.
22 Shen B, Yi X, Sun Y, Bi X, Du J, Zhang C, *et al*. Proteomic and metabolomic characterization of COVID-19 patient sera. *Cell* 2020; **182**:59–72.e15.
23 Satija R, Farrell JA, Gennert D, Schier AF, Regev A. Spatial reconstruction of single-cell gene expression data. *Nat Biotechnol* 2015; **33**:495–502.
24 Aran D, Looney AP, Liu L, Wu E, Fong V, Hsu A, *et al*. Reference-based analysis of lung single-cell sequencing reveals a transitional profibrotic macrophage. *Nat Immunol* 2019; **20**:163–172.
25 Hu C, Li T, Xu Y, Zhang X, Li F, Bai J, *et al*. CellMarker 2.0: an updated database of manually curated cell markers in human/mouse and web tools based on scRNA-seq data. *Nucleic Acids Res* 2023; **51**:D870–D876.
26 Zhang H, Meltzer P, Davis S. RCircos: an R package for Circos 2D track plots. *BMC Bioinf* 2013; **14**:244.
27 Safran M, Dalah I, Alexander J, Rosen N, Iny Stein T, Shmoish M, *et al*. GeneCards Version 3: the human gene integrator. *Database (Oxford)* 2010; **2010**:baq020.
28 Yu G. Gene ontology semantic similarity analysis using gosemsim. *Methods Mol Biol* 2020; **2117**:207–215.
29 Thrane K, Winge MCG, Wang H, Chen L, Guo MG, Andersson A, *et al*. Single-cell and spatial transcriptomic analysis of human skin delineates intercellular communication and pathogenic cells. *J Invest Dermatol* 2023; **143**:2177–2192.e13.
30 Ru Y, Kechris KJ, Tabakoff B, Hoffman P, Radcliffe RA, Bowler R, *et al*. The multiMiR R package and database: integration of microRNA-target interactions along with their disease and drug associations. *Nucleic Acids Res* 2014; **42**:e133.

31 Kariuki D, Asam K, Aouizerat BE, Lewis KA, Florez JC, Flowers E. Review of databases for experimentally validated human microRNA-mRNA interactions. *Database (Oxford)* 2023; **2023**:baad014.
32 Zhao M, Feng J, Tang L. Competing endogenous RNAs in lung cancer. *Cancer Biol Med* 2021; **18**:1–20.
33 Li Y, He Y, Chen S, Wang Q, Yang Y, Shen D, *et al*. S100A12 as biomarker of disease severity and prognosis in patients with idiopathic pulmonary fibrosis. *Front Immunol* 2022; **13**:810338.
34 Kuleshov MV, Jones MR, Rouillard AD, Fernandez NF, Duan Q, Wang Z, *et al*. Enrichr: a comprehensive gene set enrichment analysis web server 2016 update. *Nucleic Acids Res* 2016; **44**:W90–W97.
35 Roseti C, Fucile S, Lauro C, Martinello K, Bertollini C, Esposito V, *et al*. Fractalkine/CX3CL1 modulates GABAA currents in human temporal lobe epilepsy. *Epilepsia* 2013; **54**:1834–1844.
36 Fabene PF, Bramanti P, Constantin G. The emerging role for chemokines in epilepsy. *J Neuroimmunol* 2010; **224**:22–27.
37 Louboutin JP, Chekmasova A, Marusich E, Agrawal L, Strayer DS. Role of CCR5 and its ligands in the control of vascular inflammation and leukocyte recruitment required for acute excitotoxic seizure induction and neural damage. *FASEB J* 2011; **25**:737–753.
38 Cerri C, Genovesi S, Allegra M, Pistillo F, Püntener U, Guglielmotti A, *et al*. The chemokine CCL2 mediates the seizure-enhancing effects of systemic inflammation. *J Neurosci* 2016; **36**:3777–3788.
39 Kim MH, Granick JL, Kwok C, Walker NJ, Borjesson DL, Curry FR, *et al*. Neutrophil survival and c-kit(+)-progenitor proliferation in *Staphylococcus aureus*-infected skin wounds promote resolution. *Blood* 2011; **2117**:3343–3352.
40 Kamimura A, Kamachi M, Nishihira J, Ogura S, Isobe H, Dosaka-Akita H, *et al*. Intracellular distribution of macrophage migration inhibitory factor predicts the prognosis of patients with adenocarcinoma of the lung. *Cancer* 2000; **89**:334–341.
41 Islam B, Stephenson J, Young B, Manca M, Buckley DA, Radford H, *et al*. The identification of blood biomarkers of chronic neuropathic pain by comparative transcriptomics. *Neuromolecular Med* 2022; **24**:320–338.
42 Li R, Ma L, Huang H, Ou S, Yuan J, Xu T, *et al*. Altered expression of CXCL13 and CXCR5 in intractable temporal lobe epilepsy patients and pilocarpine-induced epileptic rats. *Neurochem Res* 2017; **42**:526–540.
43 Kizil C, Dudczig S, Kyritsis N, Machate A, Blaesche J, Kroehne V, Brand M. The chemokine receptor *cxcr5* regulates the regenerative neurogenesis response in the adult zebrafish brain. *Neural Dev* 2021; **7**:27.
44 Von Lüttichau I, Notohamiprodjo M, Wechselberger A, Peters C, Henger A, Seliger C, *et al*. Human adult CD34- progenitor cells functionally express the chemokine receptors CCR1, CCR4, CCR7, CXCR5, and CCR10 but not CXCR4. *Stem Cells Dev* 2005; **14**:329–336.
45 Fritze J, Ginisty A, McDonald R, Quist E, Stamp E, Monni E, *et al*. Loss of Cxcr5 alters neuroblast proliferation and migration in the aged brain. *Stem Cells* 2020; **38**:1175–1187.
46 MacDonald RJ, Yen A. CXCR5 overexpression in HL-60 cells enhances chemotaxis toward CXCL13 without anticipated interaction partners or enhanced MAPK signaling. *In Vitro Cell Dev Biol Anim* 2018; **54**:725–735.
47 Korin B, Avraham S, Azulay-Debby H, Farfara D, Hakim F, Rolls A. Short-term sleep deprivation in mice induces B cell migration to the brain compartment. *Sleep* 2022; **43**:zsz222.
48 Xiong LL, Du RL, Niu RZ, Xue LL, Chen L, Huangfu LR, *et al*. Single-cell RNA sequencing reveals peripheral immunological features in Parkinson's Disease. *NPJ Parkinsons Dis* 2024; **10**:185.
49 de Toffol B. Epilepsy and psychosis. *Rev Neurol (Paris)* 2024; **180**:298–307.
50 Calvo A, Moglia C, Canosa A, Cammarosano S, Ilardi A, Bertuzzo D, *et al*. Common polymorphisms of chemokine (C-X3-C motif) receptor 1 gene modify amyotrophic lateral sclerosis outcome: a population-based study. *Muscle Nerve* 2018; **57**:212–216.
51 Lopez-Lopez A, Gamez J, Syriani E, Morales M, Salvado M, Rodríguez MJ, *et al*. CX3CR1 is a modifying gene of survival and progression in amyotrophic lateral sclerosis. *PLoS One* 2014; **9**:e96528.
52 López-López A, Gelpi E, Lopategui DM, Vidal-Taboada JM. Association of the CX3CR1-V249I Variant with Neurofibrillary Pathology Progression in Late-Onset Alzheimer's Disease. *Mol Neurobiol* 2018; **55**:2340–2349.
53 Sheridan GK, Murphy KJ. Neuron-glia crosstalk in health and disease: fractalkine and CX3CR1 take centre stage. *Open Biol* 2013; **3**:130181.
54 Limatola C, Ransohoff RM. Modulating neurotoxicity through CX3CL1/CX3CR1 signaling. *Front Cell Neurosci* 2014; **8**:229.
55 Mosher KI, Wyss-Coray T. Microglial dysfunction in brain aging and Alzheimer's disease. *Biochem Pharmacol* 2014; **88**:594–604.
56 Gu X, Li D, Wu P, Zhang C, Cui X, Shang D, *et al*. Revisiting the CXCL13/CXCR5 axis in the tumor microenvironment in the era of single-cell omics: implications for immunotherapy. *Cancer Lett* 2024; **605**:217278.
57 Nash KR, Moran P, Finneran DJ, Hudson C, Robinson J, Morgan D, Bickford PC. Fractalkine over expression suppresses α-synuclein-mediated neurodegeneration. *Mol Ther* 2015; **23**:17–23.
58 Castro-Sánchez S, García-Yagüe AJ, López-Royo T, Casarejos M, Lanciego JL, Lastres-Becker I. Cx3cr1-deficiency exacerbates alpha-synuclein-A53T induced neuroinflammation and neurodegeneration in a mouse model of Parkinson's disease. *Glia* 2018; **66**:1752–1762.
59 Zhou Y, Zhang L, Hao Y, Yang L, Fan S, Xiao Z. FKN/CX3CR1 axis facilitates migraine-Like behaviour by activating thalamic-cortical network microglia in status epilepticus model rats. *J Headache Pain* 2022; **23**:42.
60 Rana A, Musto AE. The role of inflammation in the development of epilepsy. *J Neuroinflammation* 2018; **15**:144.
61 Bellavance MA, Gosselin D, Yong VW, Stys PK, Rivest S. Patrolling monocytes play a critical role in CX3CR1-mediated neuroprotection during excitotoxicity. *Brain Struct Funct* 2015; **220**:1759–1776.
62 Subbarayan MS, Joly-Amado A, Bickford PC, Nash KR. CX3CL1/CX3CR1 signaling targets for the treatment of neurodegenerative diseases. *Pharmacol Ther* 2022; **231**:107989.
63 Ali I, Chugh D, Ekdahl CT. Role of fractalkine-CX3CR1 pathway in seizure-induced microglial activation, neurodegeneration, and neuroblast production in the adult rat brain. *Neurobiol Dis* 2015; **74**:194–203.
64 Alves M, Gil B, Villegas-Salmerón J, Salari V, Martins-Ferreira R, Arribas Blázquez M, *et al*. Opposing effects of the purinergic P2X7 receptor on seizures in neurons and microglia in male mice. *Brain Behav Immun* 2024; **120**:121–140.
65 Zhang L, Xu J, Gao J, Wu Y, Yin M, Zhao W. CD200-, CX3CL1-, and TREM2-mediated neuron-microglia interactions and their involvements in Alzheimer's disease. *Rev Neurosci* 2018; **29**:837–848.
66 Pawelec P, Ziemka-Nalecz M, Sypecka J, Zalewska T. The impact of the CX3CL1/CX3CR1 axis in neurological disorders. *Cells* 2020; **9**:2277.
67 Ha H, Debnath B, Neamati N. Role of the CXCL8-CXCR1/2 axis in cancer and inflammatory diseases. *Theranostics* 2017; **7**:1543–1588.
68 Jiang S, Li W, Song M, Liang J, Liu G, Du Q, *et al*. CXCL1-CXCR2 axis mediates inflammatory response after sciatic nerve injury by regulating macrophage infiltration. *Mol Immunol* 2024; **169**:50–65.
69 Laffranchi M, Schioppa T, Sozio F, Piserà A, Tiberio L, Salvi V, *et al*. Chemerin in immunity. *J Leukoc Biol* 2024; **117**:qiae181.
70 Yin W, Li Y, Song Y, Zhang J, Wu C, Chen Y, *et al*. CCRL2 promotes antitumor T-cell immunity via amplifying TLR4-mediated immunostimulatory macrophage activation. *Proc Natl Acad Sci U S A* 2021; **118**:e2024171118.
71 Zhang C, Tan G, Zhang Y, Zhong X, Zhao Z, Peng Y, *et al*. Comprehensive analyses of brain cell communications based on multiple scRNA-seq and snRNA-seq datasets for revealing novel mechanism in neurodegenerative diseases. *CNS Neurosci Ther* 2023; **29**:2775–2786.
72 Song G, Shi Y, Meng L, Ma J, Huang S, Zhang J, *et al*. Single-cell transcriptomic analysis suggests two molecularly subtypes of intrahepatic cholangiocarcinoma. *Nat Commun* 2022; **13**:1642.
73 Szulzewsky F, Pelz A, Feng X, Synowitz M, Markovic D, Langmann T, *et al*. Glioma-associated microglia/macrophages display an expression profile different from M1 and M2 polarization and highly express Gpnmb and Spp1. *PLoS One* 2015; **10**:e0116644.
74 Broad LM, Sanger HE, Mogg AJ, Colvin EM, Zwart R, Evans DA, *et al*. Identification and pharmacological profile of SPP1, a potent, functionally selective and brain penetrant agonist at muscarinic M(1) receptors. *Br J Pharmacol* 2019; **176**:110–126.
75 Wang Y, Xiang X, Chen H, Zhou L, Chen S, Zhang G, *et al*. Intratumoral erythroblastic islands restrain anti-tumor immunity in hepatoblastoma. *Cell Rep Med* 2023; **4**:101044.
76 Wang M, Cai Y, Peng Y, Xu B, Hui W, Jiang Y. Exosomal LGALS9 in the cerebrospinal fluid of glioblastoma patients suppressed dendritic cell antigen presentation and cytotoxic T-cell immunity. *Cell Death Dis* 2020; **11**:896.
77 Lee C, *et al*. Galectin-9 mediates the functions of microglia in the hypoxic brain tumor microenvironment. *Cancer Res* 2024; **84**:3788–3802.
78 Liang T, Wang X, Wang F, Feng E, You G. Galectin-9: a predictive biomarker negatively regulating immune response in glioma patients. *World Neurosurg* 2019; **132**:e455–e462.
79 Tan Z, Zhang Z, Yu K, Yang H, Liang H, Lu T, *et al*. Integrin subunit alpha V is a potent prognostic biomarker associated with immune infiltration in lower-grade glioma. *Front Neurol* 2022; **13**:964590.
80 Bittner S, Knoll G, Ehrenschwender M. Death receptor 3 signaling enhances proliferation of human regulatory T cells. *FEBS Lett* 2017; **591**:1187–1195.

81 Li D, Silverberg MS, Haritunians T, Dubinsky MC, Landers C, Stempak JM, *et al*. TNFRSF1B is associated with ANCA in IBD. *Inflamm Bowel Dis* 2016; **22**:1346–1352.
82 Mukhtar I. Inflammatory and immune mechanisms underlying epileptogenesis and epilepsy: from pathogenesis to treatment target. *Seizure* 2020; **82**:65–79.
83 Sun Y, Wen Y, Wang L, Wen L, You W, Wei S, *et al*. Therapeutic opportunities of interleukin-33 in the central nervous system. *Front Immunol* 2021; **12**:654626.
84 Gao Y, Luo C, Yao Y, Huang J, Fu H, Xia C, *et al*. IL-33 alleviated brain damage via anti-apoptosis, endoplasmic reticulum stress, and inflammation after epilepsy. *Front Neurosci* 2020; **14**:898.
85 Rawat C, Kukal S, Dahiya UR, Kukreti R. Cyclooxygenase-2 (COX-2) inhibitors: future therapeutic strategies for epilepsy management. *J Neuroinflammation* 2019; **16**:197.
86 Bauer J, Vezzani A, Bien CG. Epileptic encephalitis: the role of the innate and adaptive immune system. *Brain Pathol* 2012; **22**:412–421.
87 Zhu X, Yao Y, Yang J, Zhengxie J, Li X, Hu S, *et al*. COX-2-PGE(2) signaling pathway contributes to hippocampal neuronal injury and cognitive impairment in PTZ-kindled epilepsy mice. *Int Immunopharmacol* 2020; **87**:106801.
88 Anderson G, Maes M, Berk M. Inflammation-related disorders in the tryptophan catabolite pathway in depression and somatization. *Adv Protein Chem Struct Biol* 2012; **88**:27–48.
89 Thwaites DT, Anderson CM. The SLC36 family of proton-coupled amino acid transporters and their potential role in drugtransport. *Br J Pharmacol* 2011; **164**:1802–1816.
90 Pillai SM, Meredith D. SLC36A4 (hPAT4) is a high affinity amino acid transporter when expressed in Xenopus laevis oocytes. *J Biol Chem* 2011; **286**:2455–2460.
91 Boll M, Foltz M, Rubio-Aliaga I, Daniel H. A cluster of proton/amino acid transporter genes in the human and mousegenomes. *Genomics* 2003; **82**:47–56.
92 Osborn-Heaford HL, Murthy S, Gu L, Larson-Casey JL, Ryan AJ, Shi L, *et al*. Targeting the isoprenoid pathway to abrogate progression of pulmonary fibrosis. *Free Radic Biol Med* 2015; **86**:47–56.
93 Weissenrieder JS, Reilly JE, Neighbors JD, Hohl RJ. Inhibiting geranylgeranyl diphosphate synthesis reduces nuclear androgen receptor signaling and neuroendocrine differentiation in prostate cancer cell models. *Prostate* 2019; **79**:21–30.
94 Zhang H, Li X, Liao D, Luo P, Jiang X. Alpha/beta-hydrolase domain-containing 6: signaling and function in the central nervous system. *Front Pharmacol* 2021; **12**:784202.
95 He Q, Yan D, Dong W, Bi J, Huang L, Yang M, *et al*. circRNA circFUT8 upregulates Krupple-like factor 10 to inhibit the metastasis of bladder cancer via sponging miR-570-3p. *Mol Ther Oncolytics* 2020; **16**:172–187.
96 Bao X, Zhao L, Guan H, Li F. Inhibition of LCMR1 and ATG12 by demethylation-activated miR-570-3p is involved in the anti-metastasis effects of metformin on human osteosarcoma. *Cell Death Dis* 2018; **9**:611.
97 Song B, Xu C, Zhang Y, Shan Y. Circ_ATAD3B inhibits cell proliferation of breast cancer via mediating the miR-570-3p/MX2 axis. *Prev Med* 2023; **173**:107568.
98 Li T, Yu X, Zhu X, Wen Y, Zhu M, Cai W, *et al*. Vaccarin alleviates endothelial inflammatory injury in diabetes by mediating miR-570-3p/HDAC1 pathway. *Front Pharmacol* 2022; **13**:956247.
99 Mu J, Cheng X, Zhong S, Chen X, Zhao C. Neuroprotective effects of miR-532-5p against ischemic stroke. *Metab Brain Dis* 2020; **35**:753–763.
100 Shi Y, Yi Z, Zhao P, Xu Y, Pan P. MicroRNA-532-5p protects against cerebral ischemia-reperfusion injury by directly targeting CXCL1. *Aging (Albany NY)* 2021; **13**:11528–11541.
101 Wang H, Dingledine RJ, Myers SJ, Traynelis SF, Fang C, Tan Y, *et al*. Clinical development of the GluN2B-selective NMDA receptor inhibitor NP10679 for the treatment of neurologic deficit after subarachnoid hemorrhage. *J Pharmacol Exp Ther* 2024; **392**:100046.